Appendix H
FIRO Resilience Strategy

Appendix H. FIRO Resilience Strategy

H.1 Overview

Forecast Informed Reservoir Operations (FIRO) is a reservoir management strategy that better informs decisions to retain or release water by integrating additional flexibility in operation policies and rules with enhanced monitoring and improved weather and water forecasts (AMS 2021). FIRO is currently being implemented by the U.S. Army Corps of Engineers at Lake Mendocino through an updated Water Control Manual and at Lake Sonoma under planned deviations to the Water Control Manual to mitigate impacts to flood risk management, water supply reliability, and environmental conditions caused by increasing climatic variability and reductions of Eel River transfers to the Russian River watershed. This study evaluates FIRO as a long-range climate resilience strategy for the Russian River to continue to meet management objectives given the uncertainty of weather predicted with climate change. FIRO was simulated for four Global Circulation Model projections using synthetic forecasts. The results from this analysis demonstrate the robustness of FIRO as a climate resilience strategy for increasing water supply reliability at Lake Mendocino and Lake Sonoma and managing flood risk in the Russian River.

Figure H-1. Russian River Watershed

H.2 Introduction

Climate models predict significant future changes in precipitation patterns that will likely result in increased variability of hydrology in the Russian River Watershed both seasonally and interannually. These hydrologic changes are predicted to both increase the intensity flood events and, when coupled with the increased temperatures predicted with climate change, increase the severity and duration of droughts. FIRO is an important climate resilience strategy for water supply and flood risk management for the two major multi-purpose reservoirs in the Russian River Watershed: Lake Mendocino and Lake Sonoma (Figure H-1). To better understand the potential benefits to climate change resiliency that can be realized through implementation of FIRO, Sonoma Water engineering staff collaborated with Dr. Scott Steinschneider, an expert in the development of synthetic forecasts, to complete an analysis of FIRO as a viable climate resilience strategy. This technical memo describes the methods used to evaluate FIRO as a climate resilience strategy, presents results of simulations of FIRO using projected climate change hydrology, and summarizes findings of the analysis.

H.3 Background

Increasing climate variability, significant reductions in Eel River transfers through the Potter Valley Project (PVP) beginning in 2006, and experiences during the droughts of water years 2013 to 2015 and 2020 to 2022 initially motivated an evaluation of FIRO at Lake Mendocino. Sonoma Water, the Center for Western Weather and Water Extremes at Scripps Institution of Oceanography (CW3E), and the U.S. Army Corps of Engineers (USACE) examined the viability of FIRO at Lake Mendocino as a way to improve water supply without impairing flood management capacity. Further study and analysis demonstrated that FIRO can also improve flood risk management and ecosystem conditions in addition to water supply reliability.

FIRO is a reservoir management strategy that better informs decisions to retain or release water by integrating additional flexibility in operation policies and rules with enhanced monitoring and improved weather and water forecasts (AMS 2021). FIRO is a non-structural alternative that can improve the efficiency of multi-purpose reservoirs by modernizing operations through the use of state-of-the-art forecast information, without modifying existing infrastructure. The goal of FIRO at Lake Mendocino is to increase water supply reliability without reducing—and possibly by enhancing—the existing flood protection capacity of Lake Mendocino and downstream flows for fisheries habitat.

Operational decisions at Lake Mendocino are governed by rules in the USACE Coyote Valley Dam Water Control Manual (Water Control Manual). Those rules define the Lake Mendocino guide curve, which allocates available storage to a flood control pool at the top of the reservoir and a water supply pool below that. The USACE determines the schedule and amount of water released from Lake Mendocino during flood control operations when storage levels exceed the water supply storage pool. Rules of the Water Control Manual, prior to its update in 2025, required the flood control pool to be empty except during periods of high flows downstream. The Lake Mendocino watershed (and the entire Russian River watershed) experiences large variations in the annual amount and timing of precipitation, and the occurrence of a few large storms (often in the form of atmospheric rivers) can be the difference between an above average rainfall water year and a drought (Dettinger et al. 2011). Water supply capture in Lake Mendocino is sensitive to yearly timing or distribution of rainfall due to the variable water supply pool. Given the constraints of the guide curve, the lake must receive significant inflow in the spring (past March 1) to meet the minimum instream flow requirements and downstream demands for the remainder of the year: this has become increasingly challenging with the reduction in Eel River transfers beginning in 2006 and subsequent changes beginning in 2021.

To guide the Lake Mendocino FIRO project, the Lake Mendocino Steering Committee (Steering Committee) was formed in 2014 with representatives from multiple disciplines (flood, environmental and water supply managers; engineers and hydrologists: and meteorologists and atmospheric scientists) and from multiple agencies, including the following:

- USACE
- Sonoma Water
- CW3E
- National Oceanic & Atmospheric Agency
- U.S. Geological Survey
- U.S. Bureau of Reclamation
- California Department of Water Resources (DWR)

A work plan was developed by the Steering Committee (2015) to establish a framework for evaluating whether FIRO is a viable strategy to safely manage storage levels (i.e., to maintain existing flood control protection while also improving storage reliability for water supply and ecosystems).

In July 2017, the Steering Committee completed a preliminary viability assessment (PVA) of FIRO for Lake Mendocino (FIRO Steering Committee 2017). The evaluation of FIRO was enabled by the existence of daily ensemble flow forecasts throughout the Russian River watershed, produced by the California Nevada River Forecast Center (CNRFC) using the National Weather Service (NWS) Hydrologic Ensemble Forecast System (HEFS) (Demargne et al. 2014). Retrospective ensemble forecasts (i.e., hindcasts) of Lake Mendocino inflow and the downstream watersheds were generated by the CNRFC over a 26-year period from 1985 to 2010, which allowed for model simulation and evaluation of FIRO alternatives for this historical timeframe. This study found that a forecast-informed water control plan could be a viable solution to meet project goals of improving the storage reliability of Lake Mendocino for water supply and ecosystems without increasing the flood risk to downstream communities.

Based on the positive outcomes of the PVA, major deviations to the Water Control Manual were requested by the Steering Committee and approved by the USACE to implement FIRO on an interim basis for water years 2019 through 2025. These major deviations implemented an alternative evaluated in the PVA that was developed by Sonoma Water, which provides 11,650 acre-feet (ac-ft) of encroachment in the flood control pool (known as a FIRO buffer pool) between November 1 and February 14, and an early spring refill beginning on February 15. Under these major deviations, USACE operators could retain water under their discretion within this encroachment pool for water supply using FIRO decision support tools developed by Sonoma Water and CW3E, along with existing USACE procedures and protocols. However, if forecasts indicated it was unsafe, this water could be pre-released in advance of an incoming storm to the existing top of conservation level. During the past 7 years of interim implementation of FIRO through major deviations, Lake Mendocino has seen significant benefits to water supply without increasing downstream flooding. The major deviations were especially significant in water year 2020, which allowed USACE to capture an additional 11,000 ac-ft of storage. Figure H-2 shows the observed storage (blue line) at Lake Mendocino compared to simulated storage representing operations assuming the major deviations were not in place for water years 2019 through 2025 (orange line). This figure shows that the additional water captured in February 2020 likely prevented the reservoir from going dry in October 2021, given that the reservoir is fully depleted under the no major deviation scenario. The additional storage resulting from the major deviation was critical, considering water year 2021 was one of the driest years on record.

The viability of FIRO was further evaluated by the FIRO Steering Committee with the final viability assessment (FVA) that was completed in February 2021 (Jasperse et al. 2020). This study supported and expanded the results of the PVA and found that all the alternatives evaluated could meet the project objectives with varying degrees of success for different performance criteria. The FIRO alternatives analyzed in the FVA demonstrated improved water supply reliability by allowing additional water to be stored in the flood control space during the winter up to a defined encroachment level, while also reducing flood risk by using hydrologic forecasts to strategically pre-release water and draw down storage, even into the conservation space, in advance of storm events. This study also provided a review of ongoing and future research by project partners to support future improvements in reservoir operations.

Figure H-2. Actual Storage Levels in Lake Mendocino Compared to Simulated Storage Without a Major Deviation in Place for Water Years 2019 to 2025

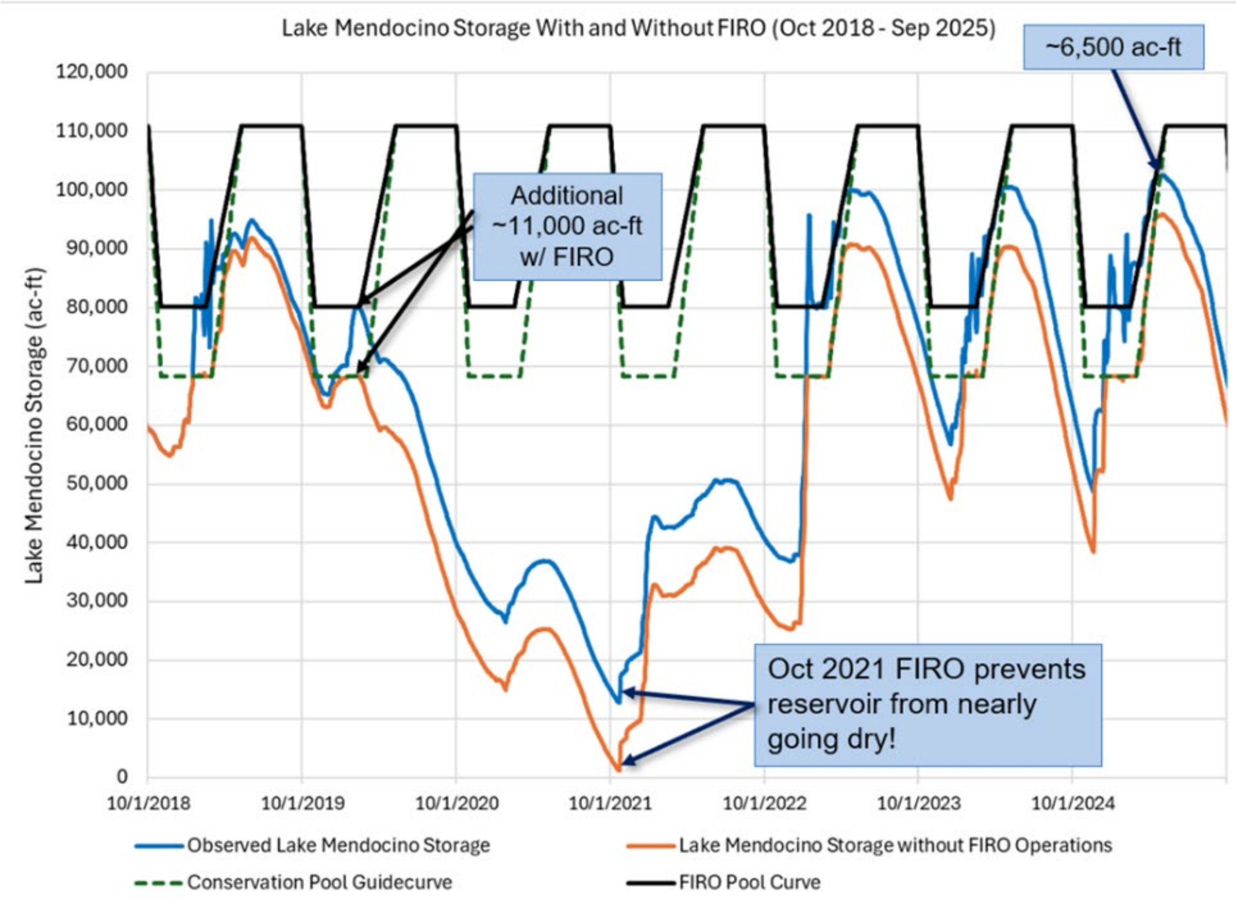

In 2022 the USACE began the studies and analyses required to update the Water Control Manual to fully implement FIRO; this was based on the benefits of FIRO demonstrated in the PVA and FVA, and years of successful interim implementation of FIRO procedures through major deviations requests. In October 2025, the updated Water Control Manual was signed and approved (USACE 2025). The FIRO buffer pool (FIRO Pool) schedule implemented in the Water Control Manual is shown on Figure H-3, which allows for encroachment above the top of conservation at the USACE's discretion of up to 11,650 ac-ft from November 1 to February 14, and a spring refill that begins on February 15 and reaches a peak conservation level of 111,000 ac-ft on May 10. The FIRO program documented in the Water Control Manual is consistent and supported with a Biological Opinion (NMFS 2025) issued by National Marine Fisheries Service in April 2025.

Based on the operational successes of FIRO at Lake Mendocino, Sonoma Water and the FIRO Steering Committee began to investigate FIRO at Lake Sonoma. In 2023, work began for the development of the Lake Sonoma FIRO Viability Assessment, which will include assessments of meteorological forecasts, hydrological forecasts, observations and monitoring, and water resources engineering. It is anticipated that this Viability Assessment will be completed in 2028 and an updated Water Control Manual that incorporates FIRO for Lake Sonoma will be completed and approved by the end of 2028.

Figure H-3. Lake Mendocino FIRO Pool Implemented in the 2025 Water Control Plan Update

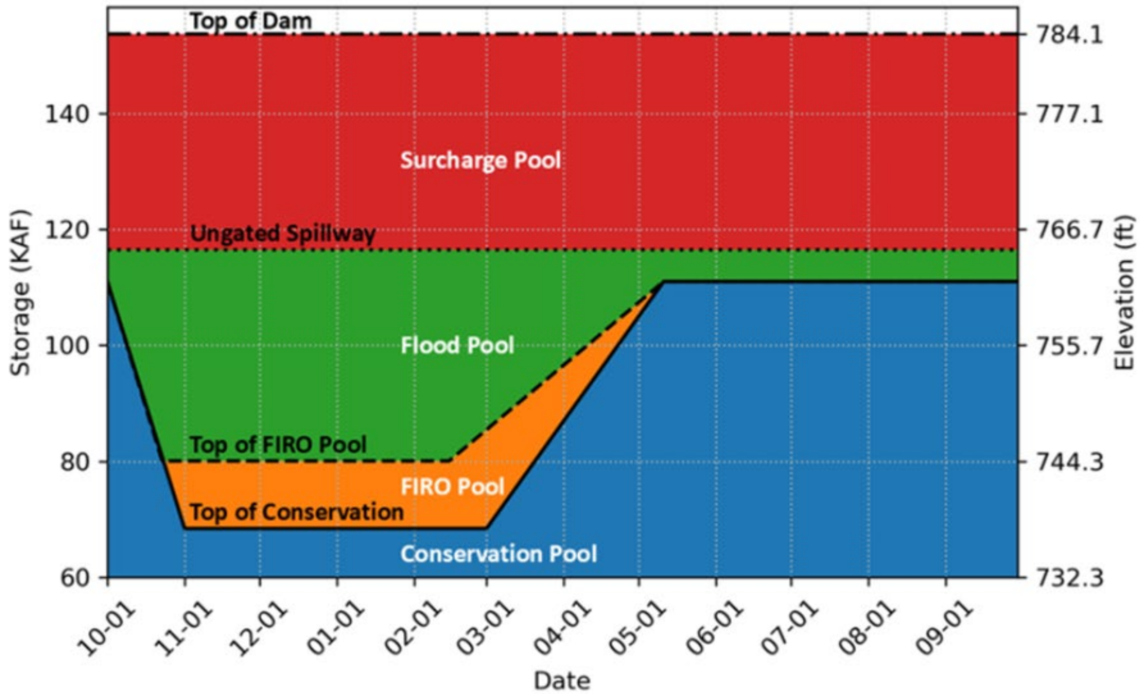

Beginning in fall 2022, Sonoma Water has requested a minor deviation for Lake Sonoma that includes the following:

- Encroachment of 9,500 ac-ft in the flood control pool from November 1 to February 14
- A spring refill that begins on February 15 and increases linearly to a level of 19,000 ac-ft on March 1
- Encroachment remaining at 19,000 ac-ft for the dry season until October 1

Each year that this minor deviation has been requested, the USACE has skillfully operated Lake Sonoma to achieve the maximum possible water supply benefit of 19,000 ac-ft.

Sonoma Water is currently working with the USACE to implement a multi-year major deviation at Lake Sonoma. If approved, this will include the same level of flood control pool encroachment as the minor deviation (9,500 ac-ft from November 1 to February 14); however, on February 15, the spring refill will increase linearly to a level of 38,100 ac-ft on March 1, and will remain at this level through the dry season until October 1. It is anticipated that this major deviation will be implemented in fall 2026 to support operations for water year 2027. Figure H-4 shows the FIRO pool schedule implemented in the multi-year minor deviation for water years 2023 through 2026 (orange shaded region) and the expanded FIRO pool to be implemented in the upcoming major deviation (red shaded region). The proposed major deviation for Lake Sonoma will establish guidelines and rules for retaining water within the FIRO pool based on forecasted information. Sonoma Water intends to request this major deviation to be in place for up to 5 years, or until it is replaced with an updated Water Control Manual that implements FIRO for Lake Sonoma.

FIRO is identified as a key climate resilience strategy for Sonoma Water's Climate Adaptation Plan (SCWA 2021) and the Russian River Watershed Resilience Pilot Project. As part of this study, Sonoma Water engineering staff evaluated the viability of FIRO as a long-term climate resilience strategy to provide water supply and flood management benefits, given the projected changes in extreme precipitation and warming with climate change.

Figure H-4. Lake Sonoma FIRO Pool with Minor and Major Deviations

(Implemented in the minor deviation for water years 2023 through 2026, and the proposed major deviation for water year 2027)

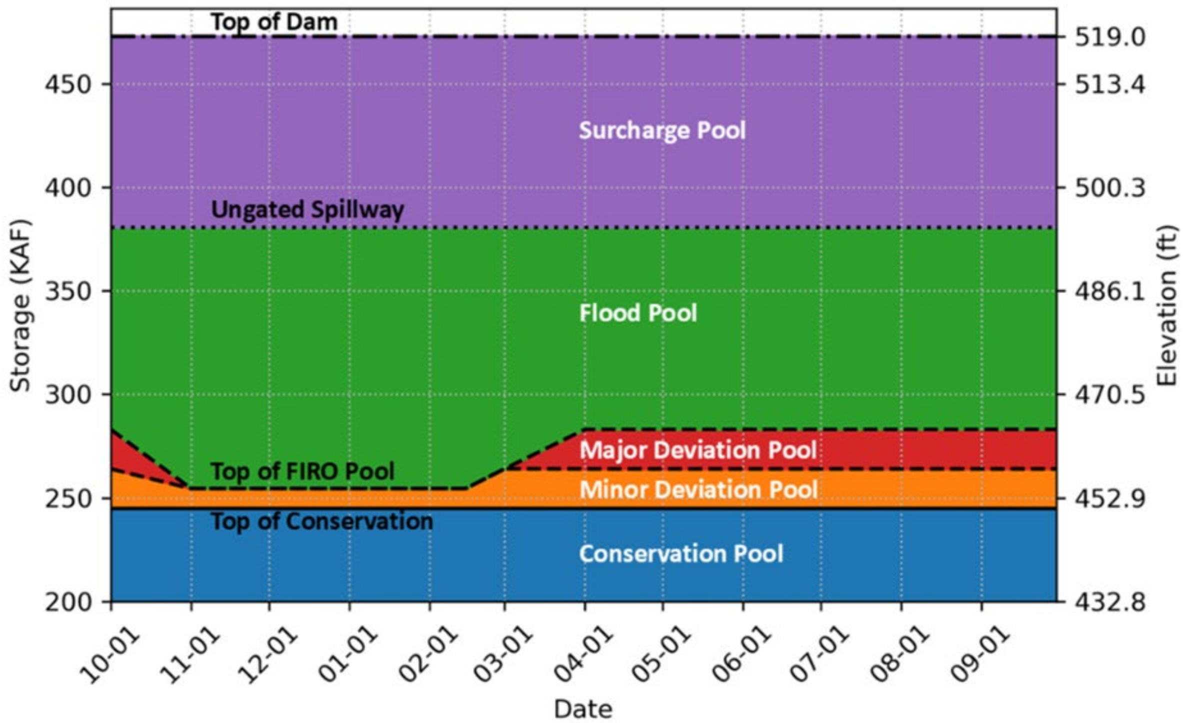

H.4 Technical Approach to Evaluate FIRO as a Climate Resilience Strategy

To evaluate FIRO as a climate resilience strategy, four Global Circulation Model (GCM) climate futures for selected shared socioeconomic pathways (SSPs) were simulated:

- ACCESS-CM2 under SSP3-7.0
- CNRM-ESM2-1 SSP2-4.5
- IPSL-CM6A-LR under SSP2-4.5
- MRI-ESM2-0 under SSP3-7.0

These scenarios were selected to capture a potential range of future climates. Three of the scenarios were selected to include a dry, median, and wet future condition based on average annual rainfall; and a fourth scenario was selected that includes extreme flood events to evaluate potential shifts in flood risk with climate change. Downscaled Localized Constructed Algorithms version 2 precipitation and temperature were incorporated into the U.S. Geological Survey Basin Characterization Model to simulate daily average hydrology under the four selected climate scenarios for the period 1950 to 2100. The 1950 to 2020 simulation period for each scenario is designed to simulate hydrology that is representative of historical climate, and the 2020 to 2100 period is designed to simulate future climate.

Typically, FIRO is simulated for a historical hydrologic period (1990 to 2023) using hindcasts of the HEFS from the NWS, which represent current forecasting bias, skill, and reliability. For this analysis, FIRO simulations were performed using hydrology derived from GCM projections. Consequently, NWS hindcasts developed for the Russian River watershed cannot be applied because the simulated hydrology has not occurred. To simulate FIRO for the four GCM scenarios, synthetic forecasts were generated by Dr. Scott Steinschneider, based on the statistical structure of forecast skill, bias, and ensemble spread of the historical HEFS hindcasts. The development of the synthetic forecasts is described in the attached memo (Attachment H-1). The development of the synthetic forecasts is a stochastic process; therefore, 20 synthetic forecast realizations were developed for each of the four climate scenarios to capture a range of plausible forecast errors. Each of the 20 synthetic forecasts includes a forecast initialization for each day of the climate scenario, with 44 ensemble members of daily average flows out to a 15-day lead time.

To simulate reservoir operations under FIRO, a reservoir operations model was employed that uses climate scenario hydrology and the synthetic forecasts to simulate reservoir releases consistent with current FIRO operational procedures. This model is called the Ensemble Forecast Operations (EFO) model (Delaney et al. 2020) and was developed by Sonoma Water to support the simulation and analysis of FIRO for the Lake Mendocino FIRO PVA and FVA described herein. Based on its success in Lake Mendocino, this model was used to support the analysis of FIRO at other reservoirs including Prado Dam, Lake Oroville, New Bullards Bar, Seven Oaks Reservoir, and Lake Sonoma (Delaney et al. 2020). Additionally, this model is currently used as one of the primary decision support tools to support real time flood control operations by the USACE in the Russian River Watershed.

The Russian River EFO model includes nine model junctions that align with the HEFS forecast locations provided by the CNRFC, which are shown on Figure H-5. These junctions include Lake Mendocino; Lake Sonoma; and flood-prone river locations including Hopland, Healdsburg, and the Hacienda Bridge near the City of Guerneville. The model includes all reservoir operational constraints such as physical storage and release capacities, maximum release schedules, and water supply operations defined in Sonoma Water's water right permits and State Water Resources Control Board Decision 1610. The model uses unimpaired hydrology from the four climate scenarios, along with the synthetic forecasts, to simulate reservoir operations and downstream flows at a daily timestep.

Figure H-5. Russian River Ensemble Forecast Operations Model Network

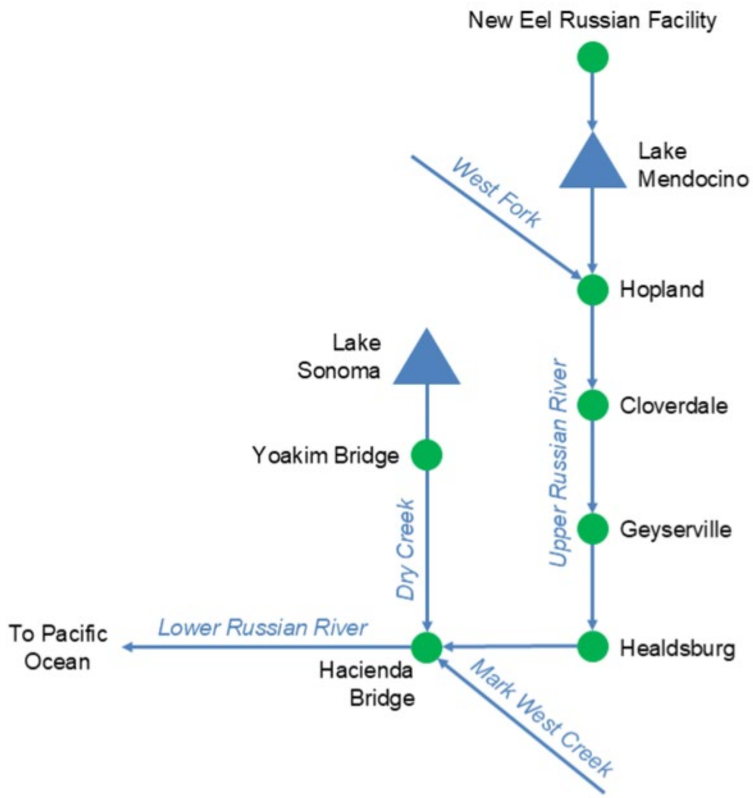

For diversions from the Eel River, all simulations assume that the PVP is decommissioned and a new run of the river facility, the New Eel Russian Facility (NERF), is operational. The model assumes that diversions from the Eel River to the east branch of the Russian River are made through this facility when flows on the Eel meet criteria defined in the *Water Diversion Agreement for the New Eel-Russian Facility* (CDFW et al. 2025) and there is space available in Lake Mendocino to store diversions. The assumptions for the NERF are applied for the entire simulation period (1950 to 2100) for all four of the GCM climate scenarios.

FIRO was simulated at Lake Mendocino, assuming the FIRO pool defined in the 2025 updated Water Control Manual (Figure H-3). Simulation of FIRO at Lake Sonoma assumed the proposed major deviation pool (Figure H-4) that will be requested to begin in water year 2027. Based on the findings of Dr. Steinschneider in the development of the synthetic forecasts, the FIRO reservoir rules were designed to only use synthetic forecasts of reservoir inflows when formulating release schedules. The regulation of releases from Lake Mendocino and Lake Sonoma to meet downstream flood control objective flows at Hopland (8,000 cubic feet per second [cfs] limit) and the Hacienda Bridge (35,000 cfs limit) are made based on perfect knowledge (i.e., perfect forecasts) of downstream hydrology. To approximate the real time uncertainty of managing downstream flood control objectives, a 20% buffer is assumed, which equates to a 6,400-cfs objective flow limit for Hopland and a 27,000-cfs limit for the Hacienda Bridge.

For comparison, simulations of operations without FIRO (No FIRO) were also developed. These simulations assume that the top of the conservation pool (Figures H-3 and H-4) is used to guide releases without allowing additional encroachment into the FIRO pool. When simulated storage exceeds the top of conservation, this water is released as quickly as possible while complying with all other release constraints and downstream flow objectives. As with the FIRO simulations, the regulation of releases from

Lake Mendocino and Lake Sonoma to meet downstream flood control objective flows were made based on perfect knowledge and applying a 20% buffer to account for real-time operational uncertainty.

H.5 Results

The results compare FIRO and No FIRO reservoir operations at Lake Sonoma and Lake Mendocino, using future climate hydrology to determine the effectiveness of FIRO as a climate change adaptation strategy in the Russian River. The future climate hydrology for the four selected climate change scenarios was simulated with the operations model and were analyzed for water supply, ecosystem, and flood risk management impacts using associated metrics for each objective. The model results were aggregated into three simulation time periods to assess the relative changes in conditions under future climate change: Historical (1980 to 2010), Mid-century (2030 to 2070), and Late-century (2070 to 2100).

H.5.1 Water Supply and Ecosystem Results

To assess water supply reliability and ecosystem impacts of FIRO at Lake Mendocino and Lake Sonoma, modeled reservoir storage results were analyzed for May 10 and April 1, respectively. These dates represent the earliest time in the year that the FIRO pool reaches the maximum storage amount for each reservoir; and the simulated storage levels on these dates approximate the water available in the reservoirs for the summer and fall.

Lake Mendocino May 10 and Lake Sonoma April 1 storage results for the FIRO and No FIRO alternatives are presented for the three simulation time periods on Figures H-6 and H-7. The results are aggregated for all four climate change scenarios into box plots for the three time periods to show the distribution of outcomes for each alternative. Additionally, for the FIRO alternatives, all 20 simulation results for the different stochastically generated synthetic forecast realizations are combined to show the potential range of outcomes based on forecast uncertainty. The box boundaries in the plot represent the 25th, 50th, and 75th percentiles or results; the whiskers outside the box represent 1.5 times the interquartile range; and the circles represent individual results that fall outside the 1.5 times the interquartile range.

Figure H-6. Model Results of Lake Mendocino May 10 Storage

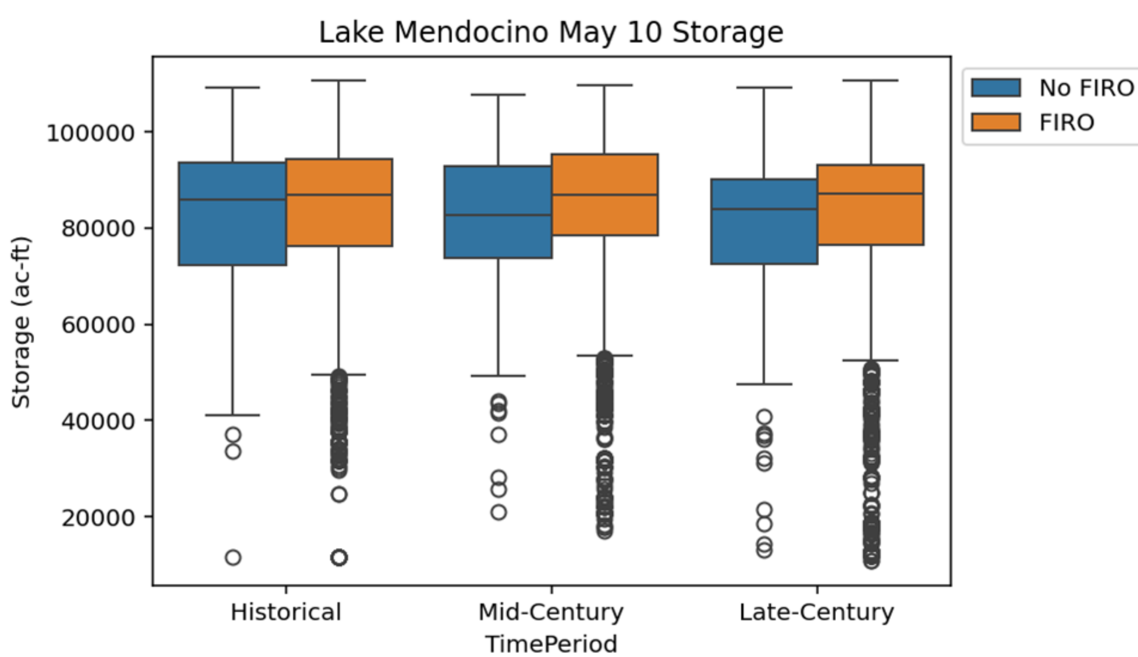

Figure H-7. Model Results of Lake Sonoma April 1 Storage

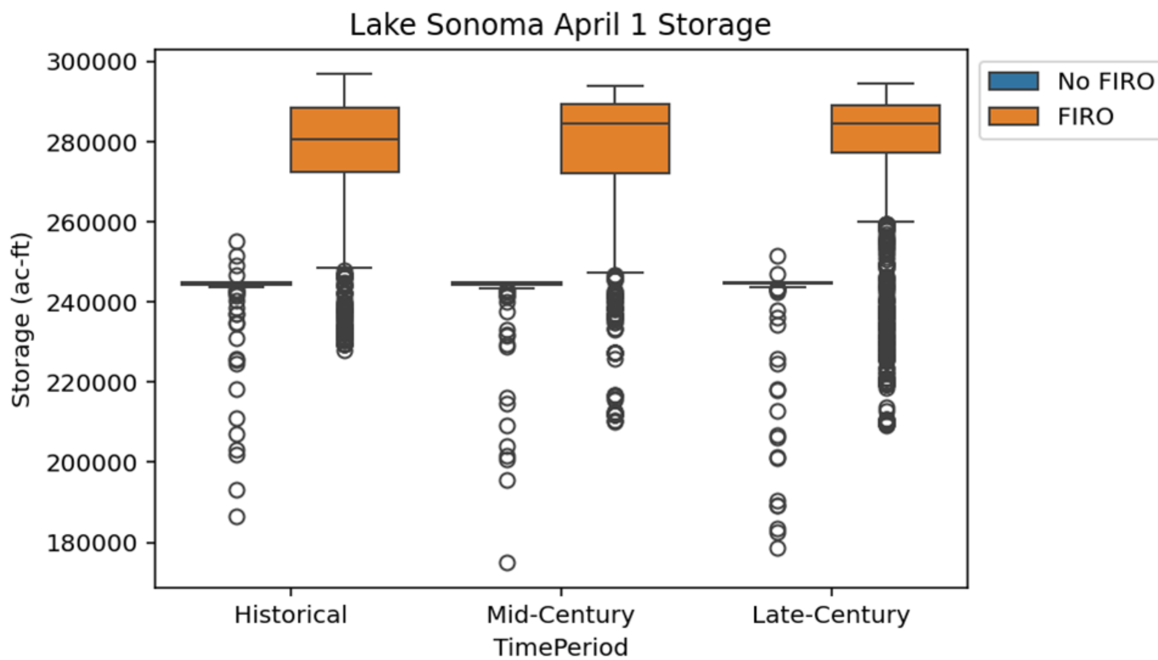

Modeled storage for both Lake Mendocino and Lake Sonoma shows an increase in water supply reliability under FIRO compared to No FIRO simulations for all time periods (Figures H-6 and H-7). Lake Mendocino shows a small increase in May 10 storage for the 50th percentile and higher ranges for all periods, while there are larger increases in storage for the 25th and lower percentile range reflecting increased drought resiliency. This indicates that FIRO has less impact on water supply reliability in the wetter years due to the convergence of the top of FIRO pool and water supply pool on May 10. The convergence means high inflows in the spring fill up the reservoir, regardless of the additional storage with the winter FIRO pool. In the drier years, represented by the bottom of the distribution, the water supply benefits are greater: the top of the FIRO pool can allow approximately 11,000 ac-ft more storage over the water supply pool in winter. This allows more winter inflows to fill up the reservoir higher and hold a higher storage going into a dry spring.

Lake Sonoma shows substantial increases in storage on April 1 with FIRO for the entire distribution of storage results and for all time periods (Figure H-7). This is due to the large FIRO pool that can allow up to 9,000 ac-ft of additional storage in the winter and up to 38,000 ac-ft of additional storage above the water supply pool from April 1 to October 31. It also appears that FIRO operations provide improved water supply benefits over the No FIRO operations in the Late-century period compared to the Historical and Mid-century periods. This benefit looks greatest in the 25th and lower percentiles due to carry-over storage from wet years to dry years. Note that there is no visible blue box for the No FIRO results on Figure H-7, because the 25%, 50%, and 75% values are approximately equal.

The increased storage at Lake Mendocino and Lake Sonoma due to FIRO supports improved water supply reliability and ecosystem health of the Russian River. The minimum instream flow requirements in the Russian River and Dry Creek are determined by Lake Mendocino storage thresholds evaluated during the spring and fall; therefore, the simulated higher storage levels in Lake Mendocino generally result in higher flows in the Russian River for improved rearing and migration conditions for salmonids. Another ecosystem benefit of higher Lake Mendocino storage is a more robust cold-water pool. The reservoir stratifies over the summer, with warmer water in the epilimnion layer floating above a colder hypolimnion pool. Since the Lake Mendocino release outlet is at the bottom of the dam, water is released from this cold-water pool until the reservoir turns over and mixes in the fall season. The timing of the turnover is affected by the storage in Lake Mendocino, with a higher storage typically corresponding to later turnover that will allow for colder water to be released into the fall when salmonids are beginning to spawn.

H.5.2 Flood Risk Management Results

To assess flood risk management impacts of FIRO under future climate conditions, three model results were analyzed: peak annual reservoir elevations, uncontrolled spill volumes, and downstream flows. Peak reservoir elevations and uncontrolled spill volumes represent risks to dam safety, because a flood management objective for Lake Mendocino and Lake Sonoma is to minimize activation of the emergency spillway. The downstream flows metric represents the change in frequency and magnitude of flood flows due to FIRO operations.

Peak water year reservoir elevations for Lake Mendocino, as provided on Figure H-8, show no increase in the whiskers for FIRO (1.5 times the interquartile range) relative to No FIRO under Historical conditions. In contrast, the whiskers and extremes are lower for FIRO than No FIRO in the Mid-century and Late-century periods, suggesting improved flood risk management. While much of the distribution below the whiskers does show an increase for FIRO relative to No FIRO, this is due to FIRO allowing more water to be stored in the reservoir at the end of a storm event to support water supply. Water Year spill volumes, as provided on Figure H-9, show no spills for both alternatives for the Historical period and show a reduction for FIRO relative to the No FIRO simulations for the Mid-century and Late-century periods. This indicates that, as storms produce more extreme precipitation in the future, the ability to pre-release and draw down storage ahead of large storms becomes more important to prevent uncontrolled releases.

Figure H-8. Model Results of Lake Mendocino Peak Annual Elevations

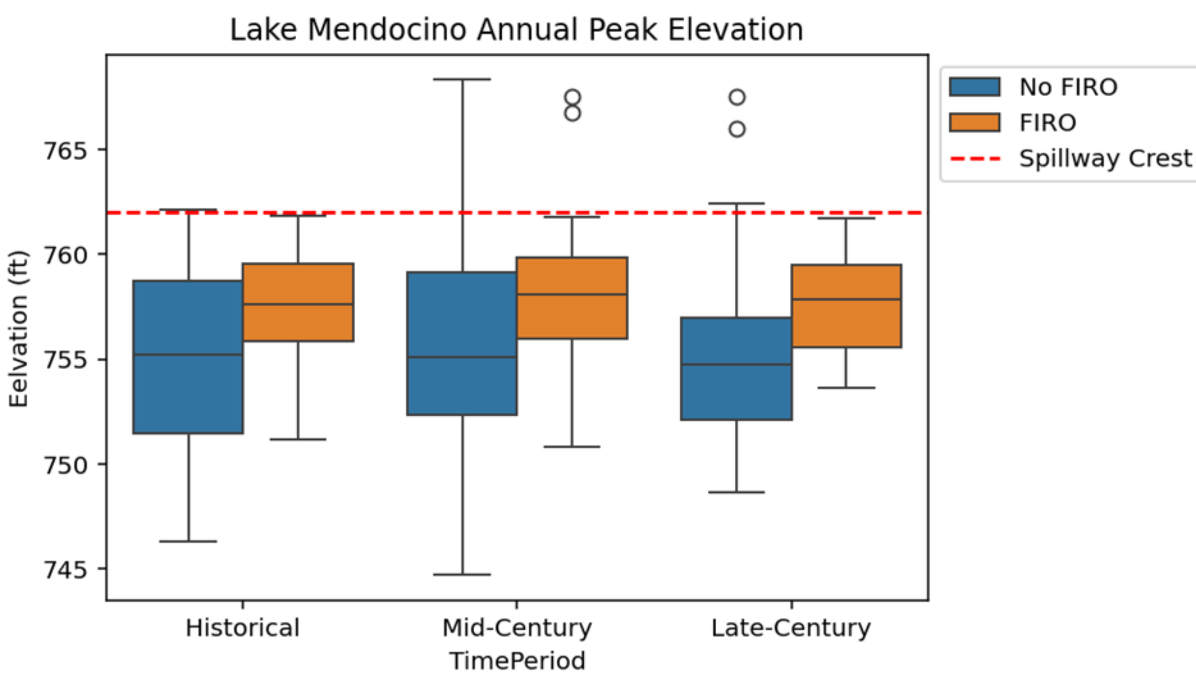

Figure H-9. Model Results of Lake Mendocino Average Water Year Spill Volumes

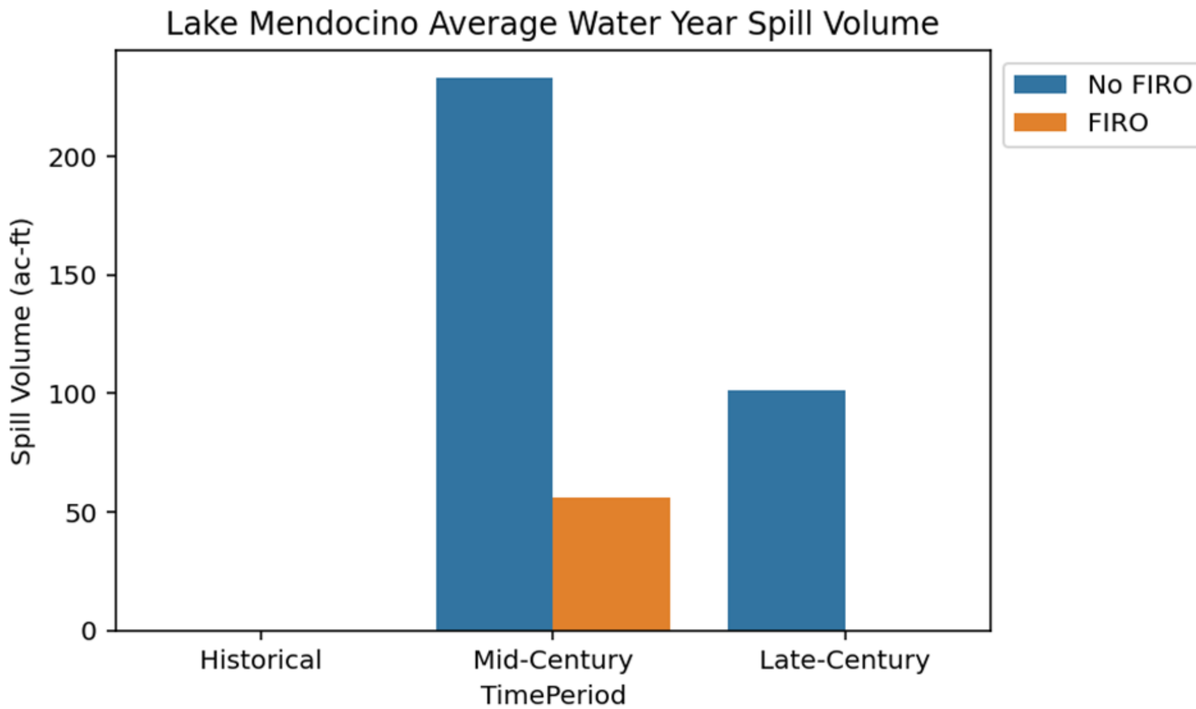

Similar to Lake Mendocino, model results for Lake Sonoma show no meaningful increase in peak water year elevations or spill volumes for FIRO relative to No FIRO for the Historical period. In the Late-century period, the most extreme peak water year elevations are slightly lower for FIRO relative to No FIRO, but neither alternative experiences spill events. However, during the Mid-century period, FIRO leads to a meaningful reduction in spill volume during the one event where peak water year elevations exceed the spillway crest (Figures H-10 and H-11). Lake Sonoma has a much larger flood pool than Lake Mendocino, so reaching the spillway crest occurs less frequently for all simulations.

Figure H-10. Model Results of Lake Sonoma Peak Annual Elevations

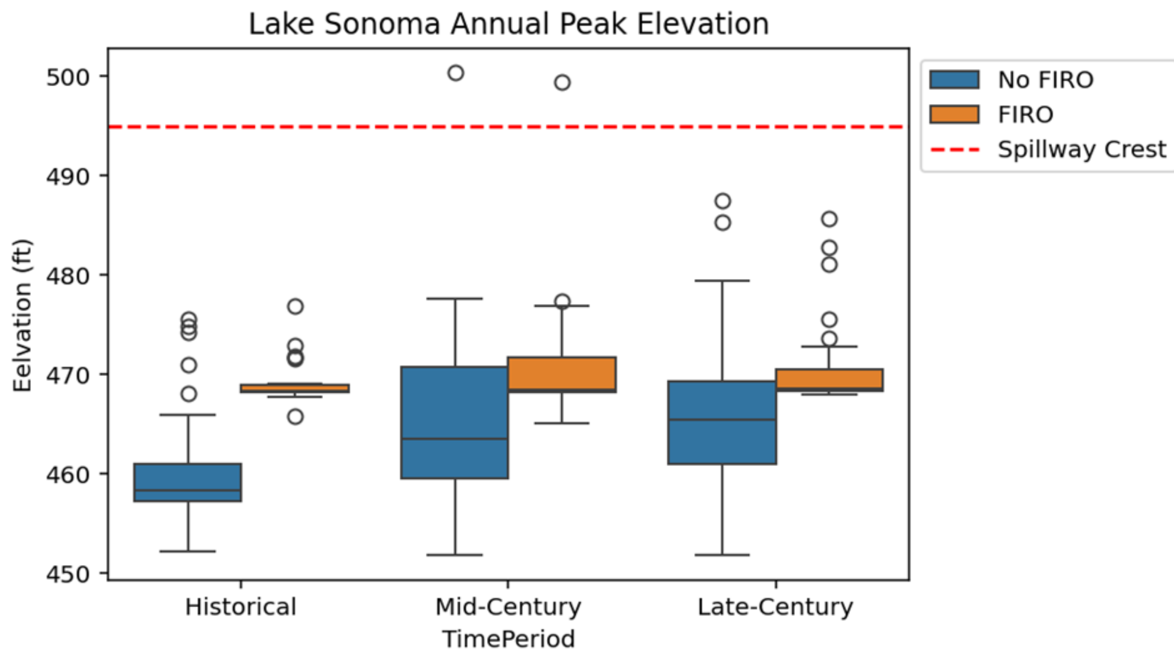

Figure H-11. Model Results of Lake Sonoma Average Water Year Spill Volumes

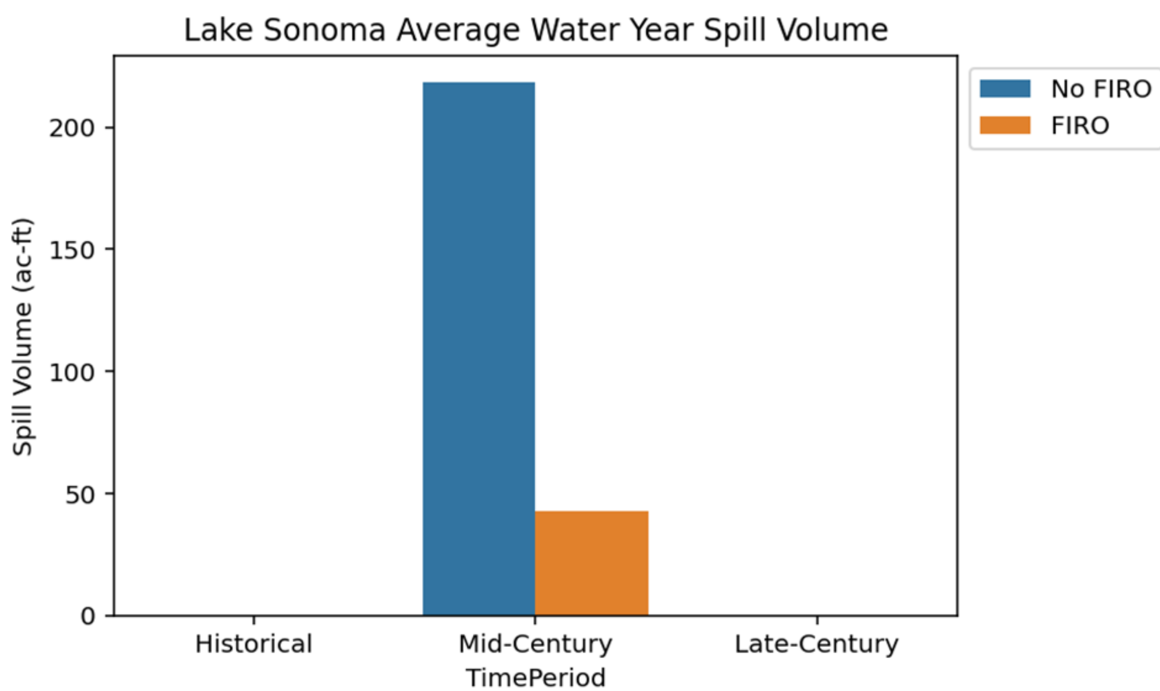

To assess the change in frequency and magnitude of flood flows for FIRO, two flow locations were analyzed: Hopland and Guerneville. The USACE operates Lake Mendocino and Lake Sonoma to minimize flows above flood stage at these locations. Peak water year flows were analyzed to determine if FIRO contributes to flooding at these locations. As shown on Figures H-12 and H-13, simulated peak water year flows at Hopland and Guerneville show very similar distributions above flood stage, as shown with the red dashed line, for both alternatives. This indicates that reservoir releases at Lake Mendocino and Lake Sonoma during FIRO operations are not impacting flood management operations during large storm events, even during more extreme events that are projected to occur in the future climate. It should also be noted from these figures that the frequency of flows above flood stage is projected to increase significantly for the Mid-century and Late-century periods for the four GCM scenarios simulated for this analysis.

Figure H-12. Model Results of Hopland Peak Water Year Flows

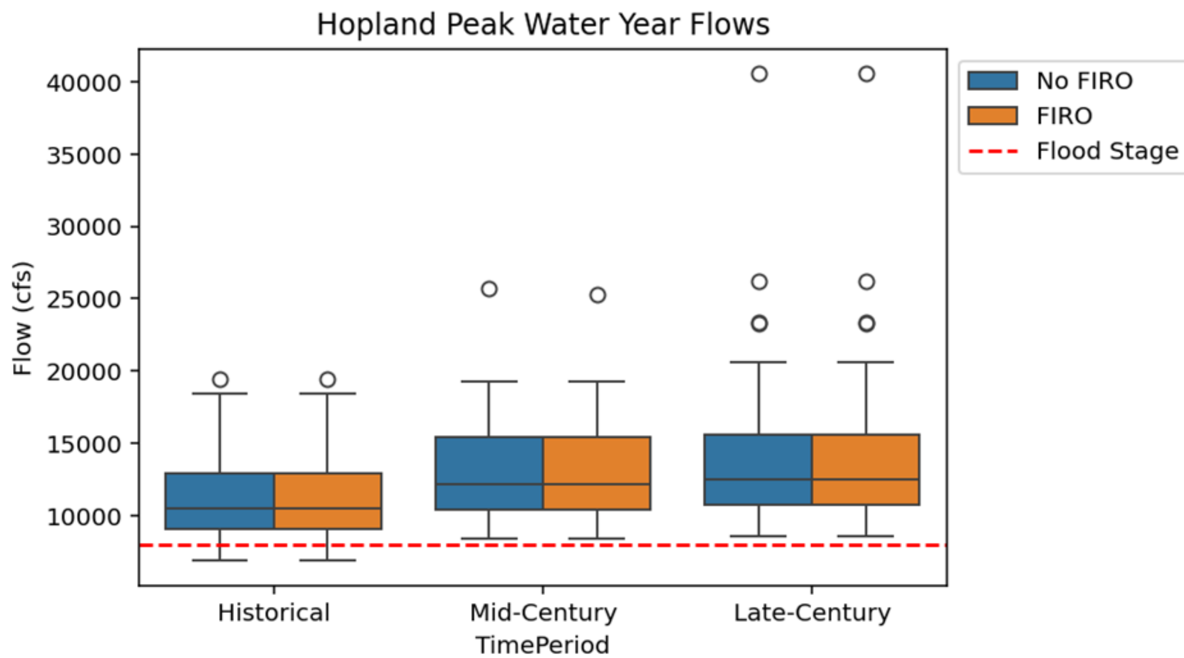

Figure H-13. Model Results of Guerneville Peak Water Year Flows

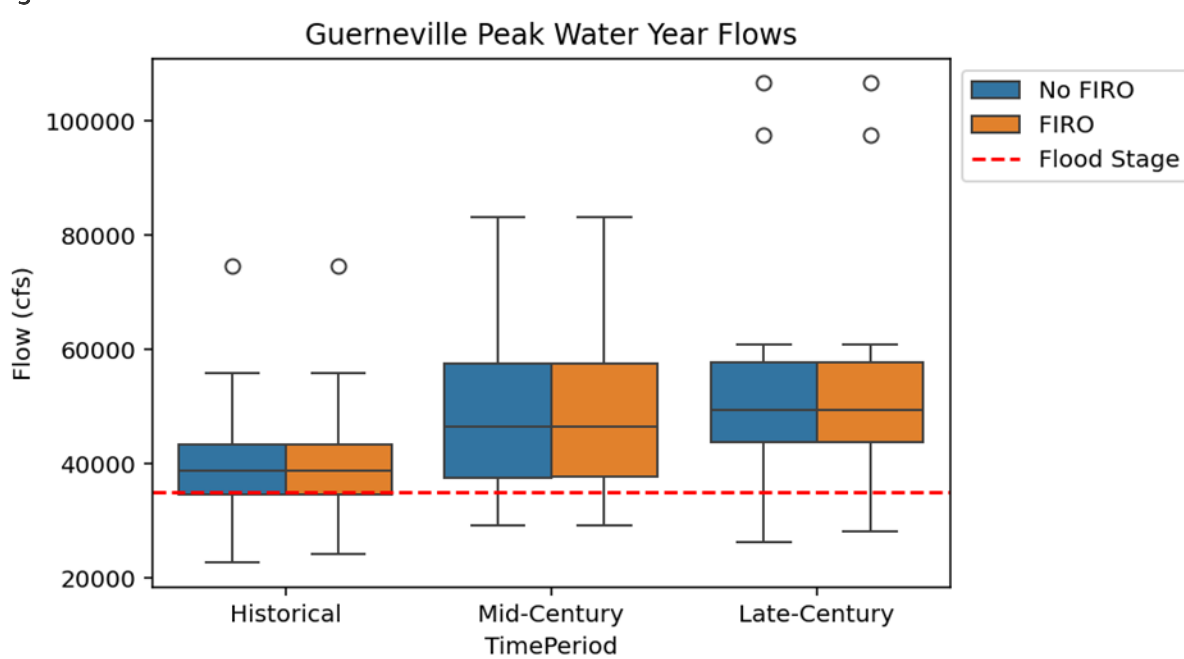

H.6 Conclusions

The Russian River is expected to experience more hydrologic extremes (droughts and floods) in the future due to climate change. Adaptation strategies must be considered for the Russian River to mitigate potential impacts to water supply, ecosystems, and flood risk. FIRO was analyzed as a climate resilience strategy to mitigate these potential impacts. The results of this analysis show that FIRO is an effective climate resilience strategy for improving water supply reliability, improving ecosystem conditions, and reducing flood risk under future climate conditions as summarized in the following:

- **Water Supply Reliability Benefits:**
  - FIRO results in higher spring storage in Lake Mendocino and Lake Sonoma compared to the No FIRO alternative, particularly in drought years.
  - The water supply reliability benefits of FIRO are maintained under climate change when comparing historical periods with future climate periods.
- **Ecosystem Benefits:**
  - Higher storage in Lake Mendocino and Lake Sonoma storage translates to higher flows during dry periods that benefit salmonid and steelhead rearing and migration.
  - Higher storage in Lake Mendocino results in a longer lasting cold-water pool that benefits salmonid spawning in the fall.
- **Flood Management Risk Benefits:**
  - Under FIRO, prereleasing into the conservation pool before a storm reduces the frequency and volume of uncontrolled spills at Lake Mendocino and Lake Sonoma for climate change conditions.
  - FIRO does not result in more downstream flooding compared to the No FIRO alternative.

H.7 References

American Meteorological Society (AMS). 2021. *Forecast-informed Reservoir Operations*. January 21. https://glossary.ametsoc.org/wiki/forecast-informed-reservoir-operations/.

California Department of Fish and Wildlife, California Trout, Eel-Russian Project Authority, County of Humboldt, Mendocino County Inland Water and Power Commission, Round Valley Indian Tribes, County of Sonoma, Sonoma County Water Agency, and Trout Unlimited (CDFW et al.). 2025. *Water Diversion Agreement for the New Eel-Russian Facility*. July.

Delaney, C. J., R.K. Hartman, J. Mendoza, M. Dettinger, L. Delle Monache, J. Jasperse Delaney et al.). 2020. "Forecast Informed Reservoir Operations Using Ensemble Streamflow Predictions for a Multipurpose Reservoir in Northern California". *Water Resources Research*, 56, e2019WR026604. https://doi.org/10.1029/2019WR026604.

Demargne, J., L. Wu, S.K. Regond, J.D. Brown, H. Lee, M. He, and J. Schaake (Demargne et al.). 2014. "The Science of NOAA's Operational Hydrologic Ensemble Forecast Service". *Bulletin of the American Meteorological Society*. 95 (1). 79–98. https://doi.org/10.1175/BAMS-D-12-00081.1.

Jasperse, J., F.M. Ralph, M. Anderson, L. Brekke, N. Malasavage, M.D. Dettinger, J. Forbis, J. Fuller, C. Talbot, R. Webb, and A. Haynes (Jasperse et al.). 2020. *Lake Mendocino Forecast Informed Reservoir Operations. Final Viability Assessment*. UC San Diego. December. https://cw3e.ucsd.edu/FIRO_docs/LakeMendocino_FIRO_FVA.pdf.

National Marine Fisheries Service (NMFS). 2025. *Endangered Species Act Section 7(a)(2) Biological Opinion and Magnuson–Stevens Fishery Conservation and Management Act Essential Fish Habitat Response for the Russian River Watershed Water Supply and Channel Maintenance Project*. April. https://repository.library.noaa.gov/view/noaa/71791.

Sonoma County Water Agency (SCWA). 2021. *Sonoma Water Climate Adaptation Plan*. October. https://www.sonomawater.org/media/PDF/Environment/Climate%20Adaptation%20Planning/SW_CAP_Final_October_2021.pdf.

U.S. Army Corps of Engineers (USACE). 2025. *Water Control Manual Coyote Valley Dam and Lake Mendocino*. Appendix I to *Master Water Control Manual, Russian River Basin, California*. U.S. Army Corps of Engineers. September.

Attachment H-1. Synthetic Forecasts for Climate Vulnerability Assessments of FIRO in the Russian River Watershed

H1.1 Introduction

This technical memo describes the development and application of synthetic ensemble streamflow forecasts to support a climate change vulnerability analysis for Sonoma Water. The synthetic forecasts are designed to emulate the statistical behavior of the operational forecasting system while allowing forecast ensembles to be generated under hydrologic conditions that extend beyond available hindcasts. In this work, synthetic forecasts were generated for 12 locations across the Russian River system, including inflows to Lake Sonoma and Lake Mendocino, as well as several additional flow points that are important for system operations and water management.

The synthetic forecasting framework is used here to provide a large set of plausible forecast sequences for evaluating reservoir operations under changing hydroclimatic conditions. By extending forecast-based operations analysis into nonstationary future conditions, the synthetic forecast ensembles provide a way to test how Forecast Informed Reservoir Operations (FIRO) may perform under a broader range of flood and water supply stressors than those represented in the historical record, including its robustness to climate change. By pairing climate-informed hydrologic stressors with synthetic forecasts that preserve key characteristics of available hindcasts, the analysis can evaluate whether FIRO continues to provide operational benefits under altered future conditions, and where vulnerabilities may emerge within the Russian River system.

H1.2 Data

The analysis uses three primary data sources, including observed daily streamflow, streamflow hindcasts, and climate projection-based daily streamflow simulations. These data provide the basis for fitting the synthetic forecasting model, evaluating its ability to reproduce historical forecast behavior, and applying it under climate-informed future hydrologic conditions.

H1.2.1 Observed Streamflow

Historical daily flows were collected for 12 locations across the Russian River system, extending from the upper watershed to Guerneville, California. These locations include inflows to Lake Sonoma (WSDC1) and Lake Mendocino (LAMC1F), as well as 10 additional flow points used in system management: BSCC1, CDLC1L, DGYC1L, GEYC1L, GUEC1L, HEAC1L, HOPC1L, MWEC1, RMKC1, and UKAC1. The observed record spans October 1, 1984, through September 30, 2023.

H1.2.2 Ensemble Hydrologic Ensemble Forecasting System Hindcasts

Historical ensemble hindcasts were obtained from the California-Nevada River Forecast Center Hydrologic Ensemble Forecasting System (HEFS) for the period October 1, 1989, through September 30, 2019. Hindcasts are available at all 12 study sites and consist of 44-member ensemble forecasts issued daily with a 15-day horizon (lead days 1 to 15). These hindcasts serve as the benchmark forecast archive used to calibrate the synthetic forecasting model and to infer the statistical structure of forecast skill, bias, and ensemble spread.

The hindcasts are based on a newer version of the Meteorological Ensemble Forecast Processor (MEFP) that incorporates conditional bias-penalized regression (Community-Based Participatory Research [CBPR];

Kim and Seo 2025). In the HEFS framework, the MEFP converts single-valued quantitative precipitation forecasts into ensemble precipitation inputs for hydrologic forecasting. The CBPR modification was introduced to better represent large events by explicitly trading a modest increase in type I error (such as false alarms or slight overprediction of smaller events) for reduced type II error (meaning fewer missed or under-forecasted large events).

The meteorological forcing used in these hindcasts varies over time. From 2012 onward, the hindcast system uses River Forecast Center quantitative precipitation forecast hindcasts for days 1 through 6 and Global Ensemble Forecast System (GEFS) hindcasts for later leads. Prior to 2012, the meteorological forecast input is based entirely on GEFS hindcasts.

H1.2.3 Climate Projection-Based Streamflow Simulations

To evaluate forecast-informed operations under nonstationary future conditions, the study also uses daily streamflow projections for all 12 sites spanning January 1, 1950, through December 31, 2100. These projected flows were developed from downscaled climate projections corresponding to four climate model-emissions combinations: ACC under SSP3-7.0, CNR under SSP2-4.5, IPS under SSP2-4.5, and MRI under SSP3-7.0. These data provide the hydrologic traces to which the synthetic forecasting model is applied, allowing synthetic ensemble forecasts to be generated under climate-informed future conditions.

H1.3 Methods

The synthetic forecasting approach used in this work is adapted from the approach in Brodeur et al. (2025). It is a nonparametric method for generating plausible ensemble inflow forecasts from a historical hindcast archive and an observed inflow record. Its purpose is to reproduce the main statistical behavior of the hindcasts while allowing many synthetic forecast realizations to be generated for periods where only observed or simulated inflow sequences are available. In broad terms, the method uses observed hydrographs as the driver; identifies similar hydrographs in the hindcast record; transfers the associated hindcast ensembles to the target event; and then rescales those ensembles so they are consistent with the magnitude and timing of the target hydrograph. This structure allows ensemble forecasts to be created for periods within the hindcast archive as well as for periods outside the hindcast period, provided an observed or reconstructed flow sequence is available. This includes future streamflow simulations under climate change.

H1.3.1 Synthetic Forecasting Algorithm

The method begins by defining a hindcast period and a generation period. The hindcast period contains both observed inflows and ensemble hindcasts (October 1, 1989 to September 30, 2019). The generation period contains the inflow sequence for which synthetic forecasts are needed. This can be set to a longer historical period for which there are inflows or a period with simulated inflows (e.g., under climate change projections).

For each forecast issue date in the generation period, the synthetic forecasting model defines a target hydrograph over the full forecast horizon (i.e., a sequence of flows from day 1 to 15). It then compares that target hydrograph against candidate hydrographs in the hindcast archive and identifies similar historical events. For the Russian River system, this analog search is driven by inflows to Lake Sonoma, which serves as the key site for matching. Similarity is computed from forward-looking observed hydrographs at that location using a weighted Euclidean distance across leads, where a parameter of the model controls how strongly different lead times contribute to the match. After these distances are computed, one analog date is drawn from the nearest neighbors, with the number of candidate neighbors another parameter of the model.

It is important to note that the final synthetic forecasts are generated for the full system (i.e., 12 locations throughout the Russian River basin; Section 2 of this report). However, the analog selection itself is anchored to Lake Sonoma inflows rather than to a multi-site distance metric. Therefore, the selected analog date represents a historical inflow event at the key site whose temporal evolution resembles the target event over the forecast window.

Once an analog date is selected, the ensemble forecast originally associated with that hindcast event is transferred to the target event and used as the basis for the synthetic forecast. A second step then rescales that resampled ensemble so it better matches the target hydrograph. This scaling is performed separately by lead time and ensemble member using the ratio between the target observed inflow and the matched hindcast observed inflow. The basic idea is to preserve the overall ensemble structure and forecast error pattern of a real historical hindcast case, while shifting the magnitude of that ensemble so it is appropriate for the event being synthesized. Conceptually, this allows the synthetic forecasting model to retain realistic features of the historical hindcasts (e.g., typical biases and spread behavior) without requiring a fully parametric stochastic error model. The method instead reuses actual ensemble structures from the hindcast archive and adapts them to new events through constrained rescaling.

A simple multiplicative scaling rule can become unstable when matched hindcast inflows are very small, since ratios involving near-zero flows can become unrealistically large. It can also produce synthetic forecasts that are too accurate at long leads if a relatively modest hindcast event is scaled too aggressively to match a much larger target event. To avoid those problems, the method constrains the allowable scaling ratio.

The first constraint depends on lead time. The allowable scaling threshold is defined by a decay curve with an upper bound, a lower bound, and a decay shape, all controlled by separate parameters in the model. This makes the scaling method more permissive at short leads and more restrictive at longer leads, which helps preserve the tendency for forecast skill to degrade with horizon. The second constraint is dependent on flow. The method transforms observed flows using a centered and scaled log transformation, then applies a sigmoid function with two parameters to further adjust the allowable scaling. This additional modifier reduces excessive scaling when target inflows are small, which is especially important for avoiding numerical instability and implausible forecast inflation under low-flow conditions.

H1.3.2 Historic Calibration

The synthetic forecasting model is calibrated directly on the hindcast period, with tunable parameters including the number of nearest neighbors, the weighting factor for lead times in the analog selection process, the lead-decay exponent for scaling, the upper and lower scaling thresholds, and the two sigmoid parameters governing the flow-dependent adjustment during scaling. These parameters are optimized numerically using differential evolution within prescribed bounds. Calibration is focused on forecasted flows to Lake Sonoma. More specifically, verification metrics for a set of verification dates targeted to major events (i.e., the largest 100 flow events) are computed at that location.

The calibration objective combined two terms. The first term measures the mean squared difference in the mean continuous rank probability score (CRPS) across lead times between hindcasts and synthetic forecasts. The second term measures the mean squared difference between hindcast and synthetic cumulative rank histograms across leads. These two terms are weighted near-equally in the objective function. This choice of objective function is designed to target both forecast accuracy and forecast reliability. That is, matching CRPS helps align the overall probabilistic performance of the synthetic ensembles with that of the hindcasts, while matching cumulative rank histograms helps reproduce reliability characteristics such as bias and dispersion across leads. The result is a synthetic forecasting model that is not just accurate in aggregate, but one that is also designed to emulate the distributional behavior of the hindcast ensemble.

H1.3.3 Application of Synthetic Forecasts to Climate Change Traces

The calibrated synthetic forecasting model is applied to climate projection-based daily streamflow sequences for all 12 sites in the Russian River system to generate forecast ensembles under future hydrologic conditions. In this step, the HEFS hindcast archive remains the basis for characterizing forecast behavior, while the climate-informed flow sequences define the target hydrographs for synthetic forecast generation. Thus, the model transfers historical forecast error structure from HEFS to climate change inflow traces using the same analog-resampling and constrained-scaling framework used in the hindcast analysis.

For each climate scenario, 20 independent synthetic forecast samples are generated, with each sample consisting of a continuous sequence of 1- to 15-day ensemble forecasts across the full climate record and across all sites. The model continues to use Lake Sonoma as the key site for analog matching, while preserving multi-site forecast generation across the broader system. Because the synthetic model is stochastic, these multiple samples represent alternative but plausible realizations of forecast evolution under the same climate scenario. This enables the climate vulnerability analysis to assess FIRO performance under future inflow conditions while accounting for realistic short-range forecast uncertainty.

H1.4 Results

H1.4.1 Historical Verification of Synthetic Forecasts

First, the ability of the synthetic forecasting model to reproduce the statistical behavior of HEFS over the hindcast period is evaluated. This verification focuses on the full set of synthetic forecasts generated for the historical record, consisting of 20 stochastic samples, each with 44 ensemble members at daily lead times from 1 to 15 days. Performance is assessed by comparing synthetic forecasts against the HEFS hindcasts using several complementary diagnostics, including distributions of CRPS by lead time, cumulative rank histograms by lead time, and visual comparisons of ensemble forecasts for selected example events. These results are shown on Figures H1-1 through H1-7 for Lake Sonoma and Lake Mendocino, with similar figures for the remaining 10 sites provided in Addendum H-1a. In Figure H1-8, the correlation of CRPS values across pairs of sites is also examined to verify that synthetic forecasts are correctly correlated spatially across the Russian River Basin.

Overall, the synthetic forecasts reproduce well the main forecast characteristics of HEFS over the hindcast period. Across leads, the CRPS distributions for the synthetic forecasts closely track those from HEFS (Figures H1-1 and H1-2; Figures H1a-1 through H1a-10), indicating that the synthetic model is able to preserve the overall level and evolution of probabilistic forecast skill with forecast horizon. Differences between the synthetic and HEFS CRPS distributions are generally modest, though some departures emerge at individual leads. For example, synthetic CRPS distributions exhibit small negative biases (i.e., too skillful) compared to HEFS for Lake Mendocino at longer leads (Figure H1-2). However, these differences are small, and some deviation is expected given the stochastic nature of the resampling procedure and the fact that the synthetic model is designed to emulate, rather than exactly reconstruct, the archived hindcasts.

Figure H1-1. Comparison of CRPS Distributions for HEFS Hindcasts and Synthetic Forecasts by Lead Time over the 100 Largest Flow Events in the Historical Hindcast Period for Lake Sonoma

(Synthetic forecasts are summarized across 20 independent stochastic samples. The solid dot shows the mean CRPS across events.)

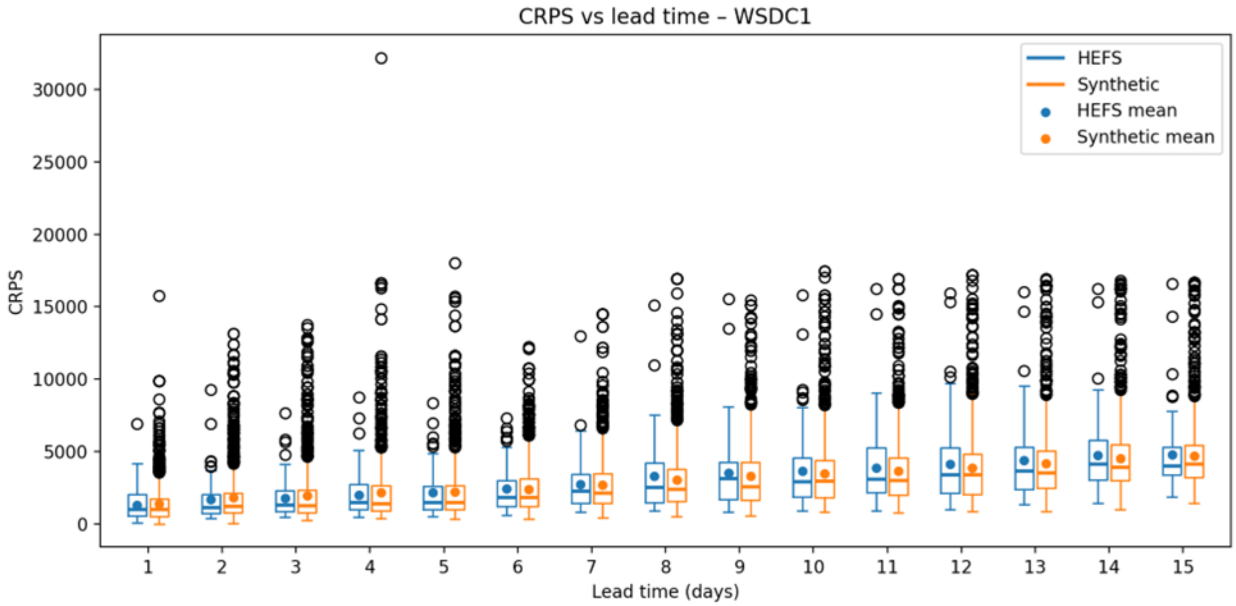

Figure H1-2. Comparison of CRPS Distributions for HEFS Hindcasts and Synthetic Forecasts by Lead Time over the 100 Largest Flow Events in the Historical Hindcast Period for Lake Mendocino

(Synthetic forecasts are summarized across 20 independent stochastic samples. The solid dot shows the mean CRPS across events.)

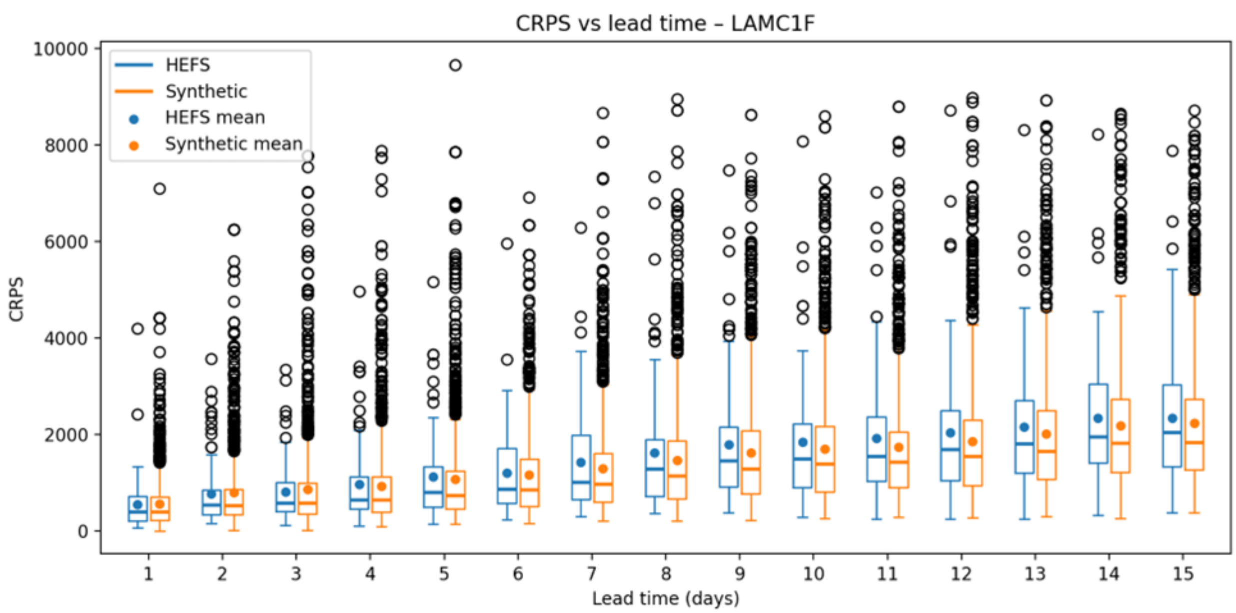

The rank histogram comparisons provide a complementary view of performance (Figures H1-2 and H1-3; Figures H1a-11 through H1a-20). These results show that the synthetic forecasts are also able to reproduce the main calibration structure of HEFS, including lead-dependent patterns in ensemble bias and reliability. In particular, the cumulative rank histograms for the synthetic forecasts follow the same general patterns seen in the hindcasts, where the ensemble is largely unbiased and reliable at short leads but becomes increasingly biased low at longer leads. This is an important result for the present application, because the synthetic forecasts are intended for operations analysis under climate stress and therefore must reflect realistic forecast uncertainty. Some discrepancies in the rank histograms at some leads likely reflect limits in the synthetic forecasting framework, but the broad agreement indicates that the synthetic model captures the dominant reliability structure of the hindcasts.

Figure H1-3. Cumulative Rank Histograms by Lead Time for HEFS Hindcasts and Synthetic Forecasts over the 100 Largest Flow Events in the Historical Hindcast Period for Lake Sonoma

(For the synthetic forecasts, a range of results are shown across 20 independent stochastic samples.)

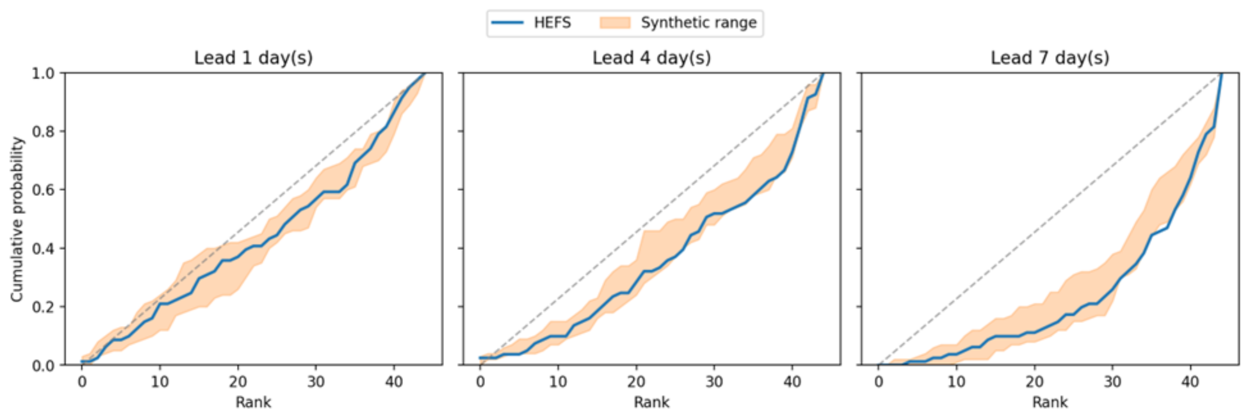

Figure H1-4. Cumulative Rank Histograms by Lead Time for HEFS Hindcasts and Synthetic Forecasts over the 100 Largest Flow Events in the Historical Hindcast Period for Lake Mendocino

(For the synthetic forecasts, a range of results are shown across 20 independent stochastic samples.)

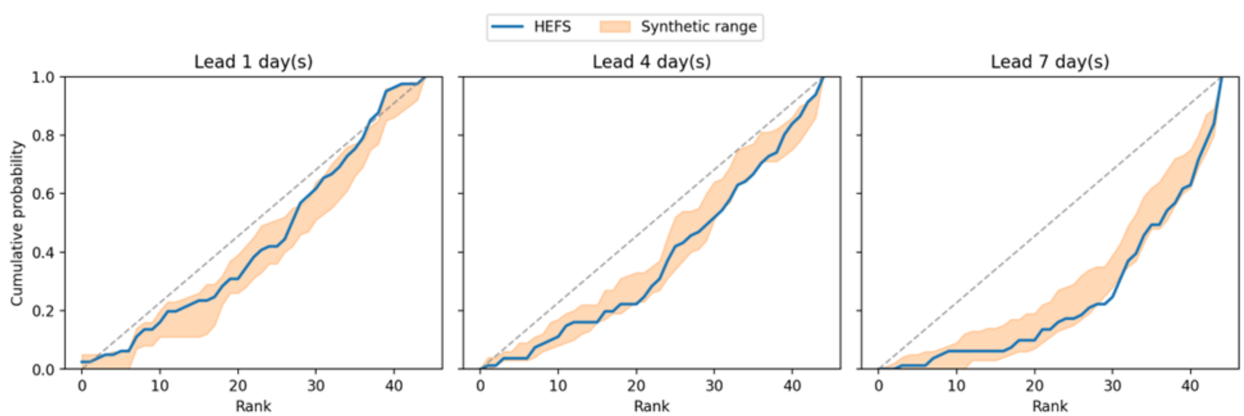

The sample flood event comparisons further illustrate how the synthetic forecasts reproduce forecast behavior during individual hydrologic events. Three events are shown, including the February 2019 peak flow at Lake Sonoma (Figure H1-5), the December 2005 flood at Lake Mendocino (Figure H1-6), and the February 1986 flood at Lake Sonoma (Figure H1-7). In Figures H1-5 and H1-6, results show that the synthetic ensembles generally capture the same features present in HEFS, including the timing of forecast evolution, the spread of the ensemble, and the tendency for skill and uncertainty to vary across lead times. Given the stochastic nature of the synthetic forecasts, we do not expect (or want) the synthetics to exhibit the same performance as HEFS for a given lead time. Rather, the synthetic samples are designed to provide alternative, plausible realizations of ensemble forecast error. For example, on Figure H1-5 (second row; third column), one synthetic sample shows the potential to pick up a forecast signal for the 2019 flood 7 days in advance, even though this event was missed at that lead time in HEFS (first row; third column). Conversely, the two synthetic samples for the 2005 flood at Lake Mendocino show the potential to miss or mistime the secondary peak of the event (Figure H1-6: second and third row; first column), even though in HEFS this secondary peak was captured reasonably well by the ensemble (Figure H1-6: first row; first column).

Figure H1-5. Example Time Series Comparison of HEFS and Synthetic Ensemble Forecasts for the February 2019 Flood into Lake Sonoma

(The top row shows the original HEFS forecasts, while the second and third rows show synthetic forecast ensembles from two different stochastic samples. Each column displays 1-, 4-, and 7-day ahead ensemble forecasts.)

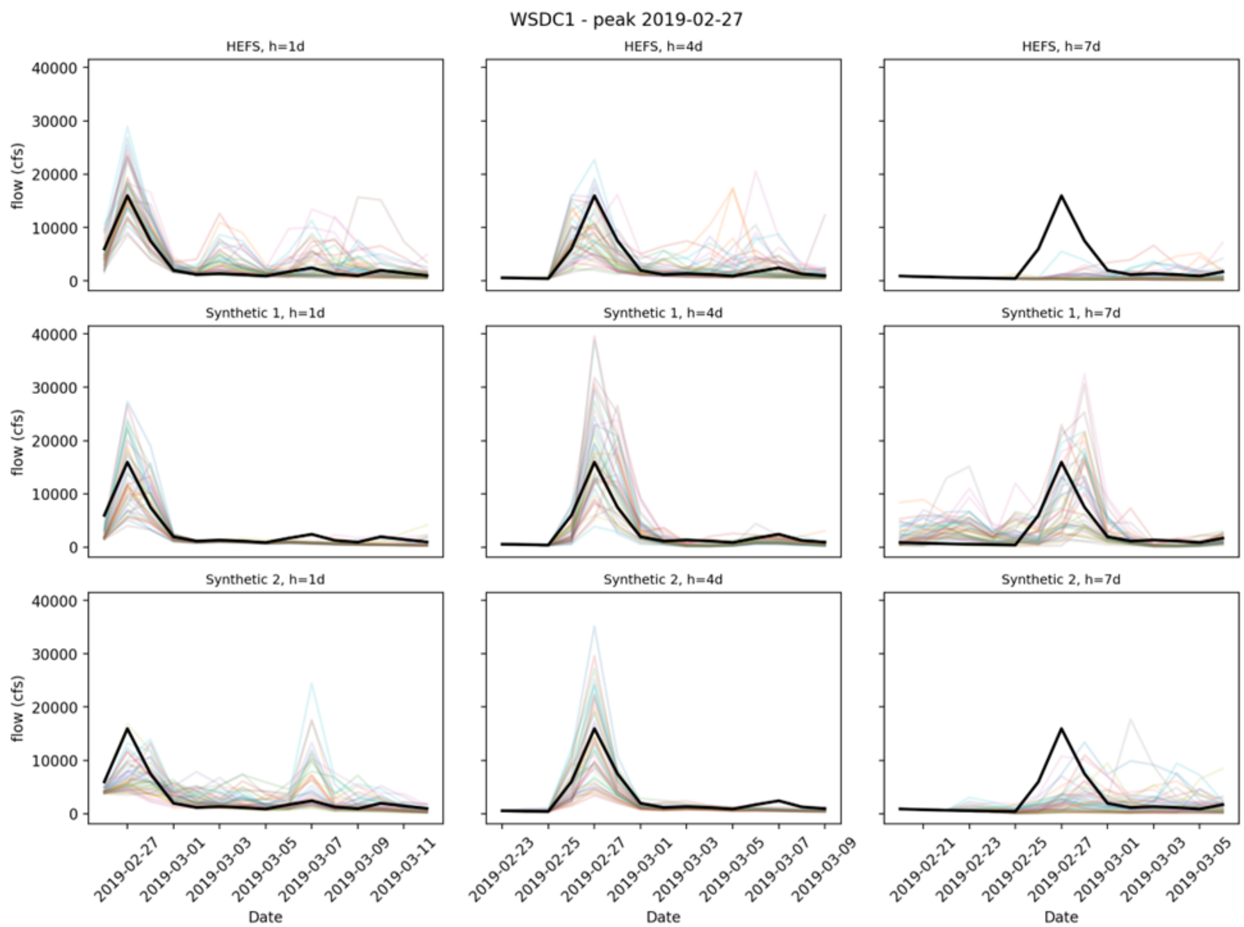

Figure H1-6. Example Time Series Comparison of HEFS and Synthetic Ensemble Forecasts for the February 2019 Flood into Lake Mendocino

(The top row shows the original HEFS forecasts, while the second and third rows show synthetic forecast ensembles from two different stochastic samples. Each column displays 1-, 4-, and 7-day ahead ensemble forecasts.)

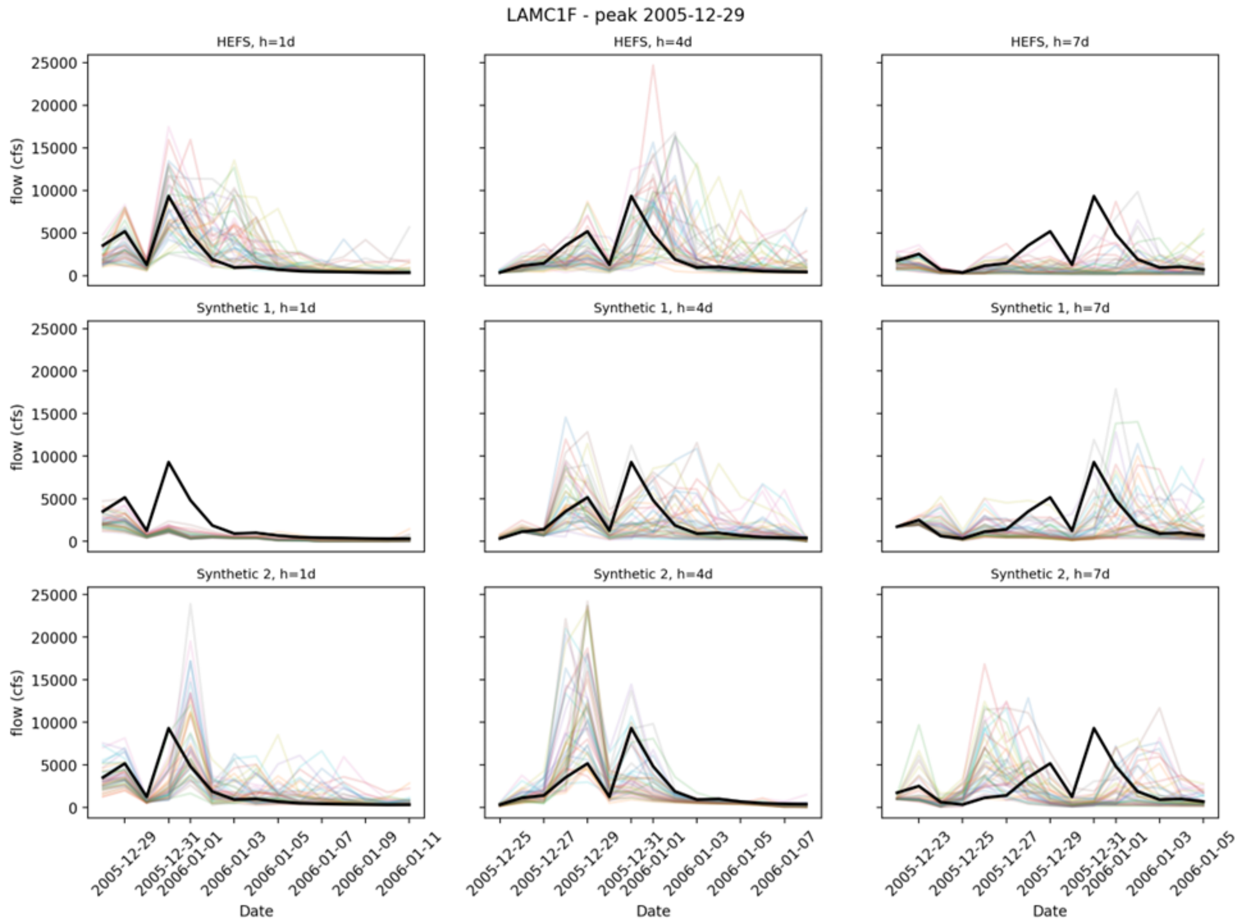

Figure H1-7 demonstrates that the synthetics can be used to extend plausible realizations of ensemble forecast error to events for which HEFS hindcasts are unavailable. For the 1986 flood, the top row of Figure H1-7 only shows the observed flows, as no HEFS hindcasts are available for this event. However, the two synthetic forecasts show very plausible forecast behavior, with good accuracy at a 1-day lead that becomes noisier at longer leads.

Figure H1-7. Example Time Series Comparison of HEFS and Synthetic Ensemble Forecasts for the February 1986 Flood into Lake Sonoma

(The top row shows only the observed flow, because there is no HEFS hindcast available for this event. The second and third rows show synthetic forecast ensembles from two different stochastic samples. Each column displays 1-, 4-, and 7-day ahead ensemble forecasts.)

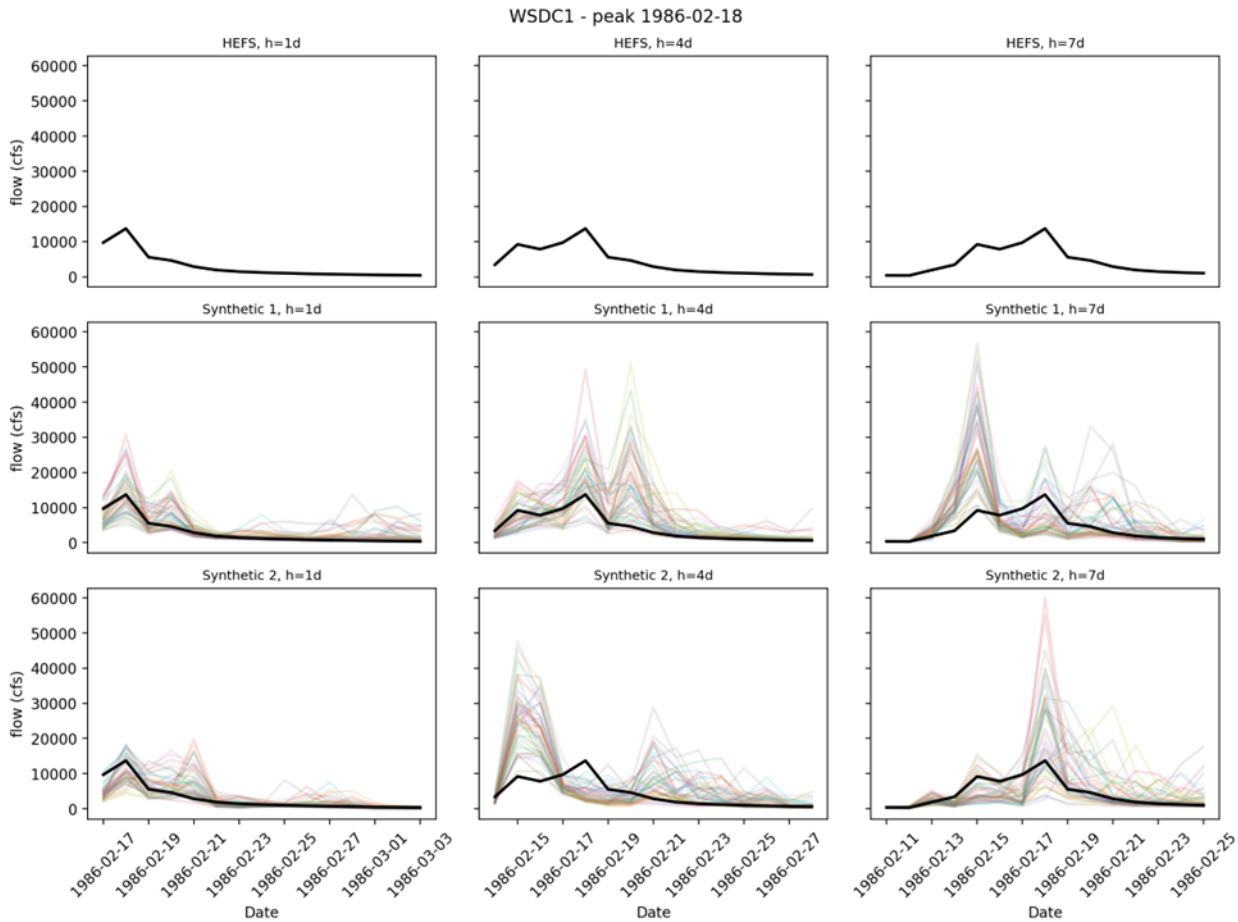

These event examples demonstrate that the synthetic forecasts behave realistically not only in aggregate across the full record, but also during specific events relevant to system operations. At the same time, the event plots make clear that the synthetic forecasts are not intended to reproduce the exact realization of any particular HEFS forecast. Rather, they are designed to generate alternative but statistically consistent forecast ensembles whose accuracy, spread, and reliability resemble those of the hindcasts.

Finally, on Figure H1-8, an evaluation is made of whether the synthetic forecasting model reproduces the spatial structure of forecast performance across the system. To do this, pairwise correlations in CRPS are compared across all site pairs for HEFS and the synthetic forecasts at each lead time. These comparisons are shown for the 66 unique site pairs among the 12 forecast locations (i.e., $66 = \binom{12}{2}$ combinations).

Figure H1-8. Pairwise Correlations in CRPS Across Sites for HEFS Hindcasts and Synthetic Forecasts, Shown Separately for Forecast Leads 1-15

(Each point represents one of the 66 unique site pairs among the 12 forecast locations, with the HEFS correlation on the x-axis and the synthetic forecast correlation on the y-axis. The dashed 1:1 line indicates perfect agreement.)

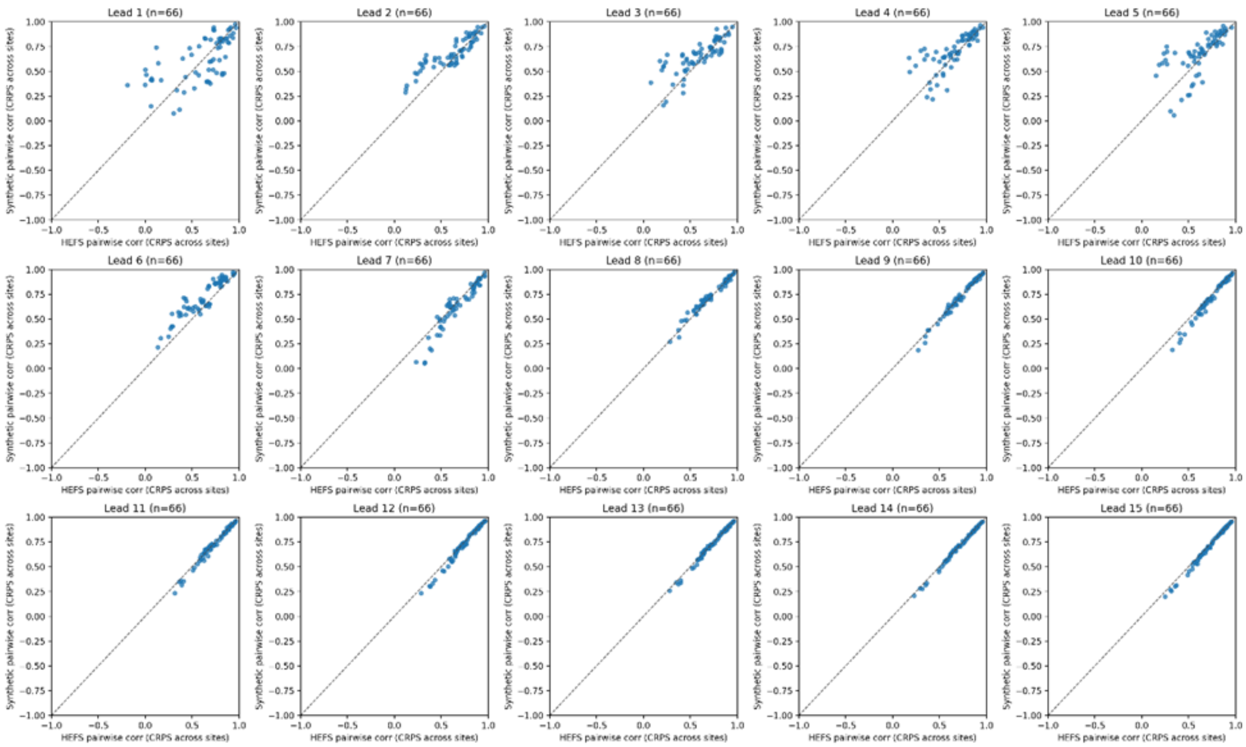

Overall, the synthetic forecasts reproduce the spatial dependence structure of HEFS forecast skill reasonably well. At nearly all leads, the pairwise CRPS correlations from the synthetic forecasts closely follow those from HEFS, with most points falling near the 1:1 line. This indicates that the synthetic model preserves the tendency for forecast performance to co-vary across locations, which is important for a multi-site operations analysis in which forecast errors at different points in the basin may occur coherently. The agreement is somewhat weaker at the shortest leads, where there is more scatter around the 1:1 line. In these early leads, the synthetic forecasts tend to reproduce the broad ranking of stronger versus weaker cross-site dependence, but not every pairwise relationship exactly. As lead time increases, however, the agreement becomes increasingly tighter; by roughly the middle to later portion of the forecast horizon (i.e., lead 8 to 15), the synthetic and HEFS correlations are very closely aligned for most site pairs.

Taken together, the results presented herein indicate that the synthetic forecasting model provides a credible emulation of HEFS over the hindcast period. The CRPS comparisons show that the approach reproduces the overall level of probabilistic forecast skill across leads, while the rank histogram comparisons show that it also preserves important features of ensemble reliability. The sample event plots reinforce that the synthetic forecasts remain realistic at the scale of individual events and can be extended to events for which hindcasts are unavailable. The CRPS correlation results indicate that the synthetic forecasts preserve how forecast accuracy co-varies across the Russian River system, which is valuable for evaluating reservoir operations and FIRO performance under basinwide hydrologic stress. Overall, this historical verification provides the basis for applying the synthetic forecasting framework to climate-informed streamflow projections, where the goal is not to recreate historical forecasts exactly, but rather to generate plausible forecast ensembles that retain the essential behavior of HEFS under altered future hydrologic conditions. The latter is described next.

H1.4.2 Synthetic Forecasts for Climate Projections

Before interpreting synthetic forecast behavior under future climate conditions, it is useful to first compare the historical baseline flows from the climate model-driven hydrologic simulation against the observed flow record. This comparison is important because the synthetic forecasting model transfers a forecast error structure learned from HEFS onto modeled streamflow. As a result, if the baseline modeled hydrology differs from observations, then the resulting synthetic forecast skill distributions may also differ from HEFS, even before any future climate change signal is introduced.

Figure H1-9 compares water-year annual peak flow distributions at all 12 sites between observed flows and one of the baseline simulations (MRI: SSP3-7.0) over the historical (1950 to 2020) period. Results for the other climate model scenarios are very similar (not shown). At several locations, the modeled and observed annual peak distributions are reasonably similar in their overall range and shape. This is the case at BSCC1, CDLC1L, GUEC1L, MWEC1, UKAC1, LAMC1F, and WSDC1, where the MRI baseline reproduces the observed peak flow distribution fairly well (despite some underestimation of the largest peaks). At other sites, however, the differences are more substantial. For example, at DGYC1L, GEYC1L, HEAC1L, HOPC1L, and RMKC1, the modeled annual peak flow distribution is shifted toward much smaller values and appears more compressed than the observed distribution.

Figure H1-9. Distribution of Water-year Annual Peak Flows at the 12 Study Sites for Observed Flows and the Historical Baseline Portion of the MRI-driven Hydrologic Simulation

(The observed record spans 1984–2023, while the modeled baseline record spans 1950–2020)

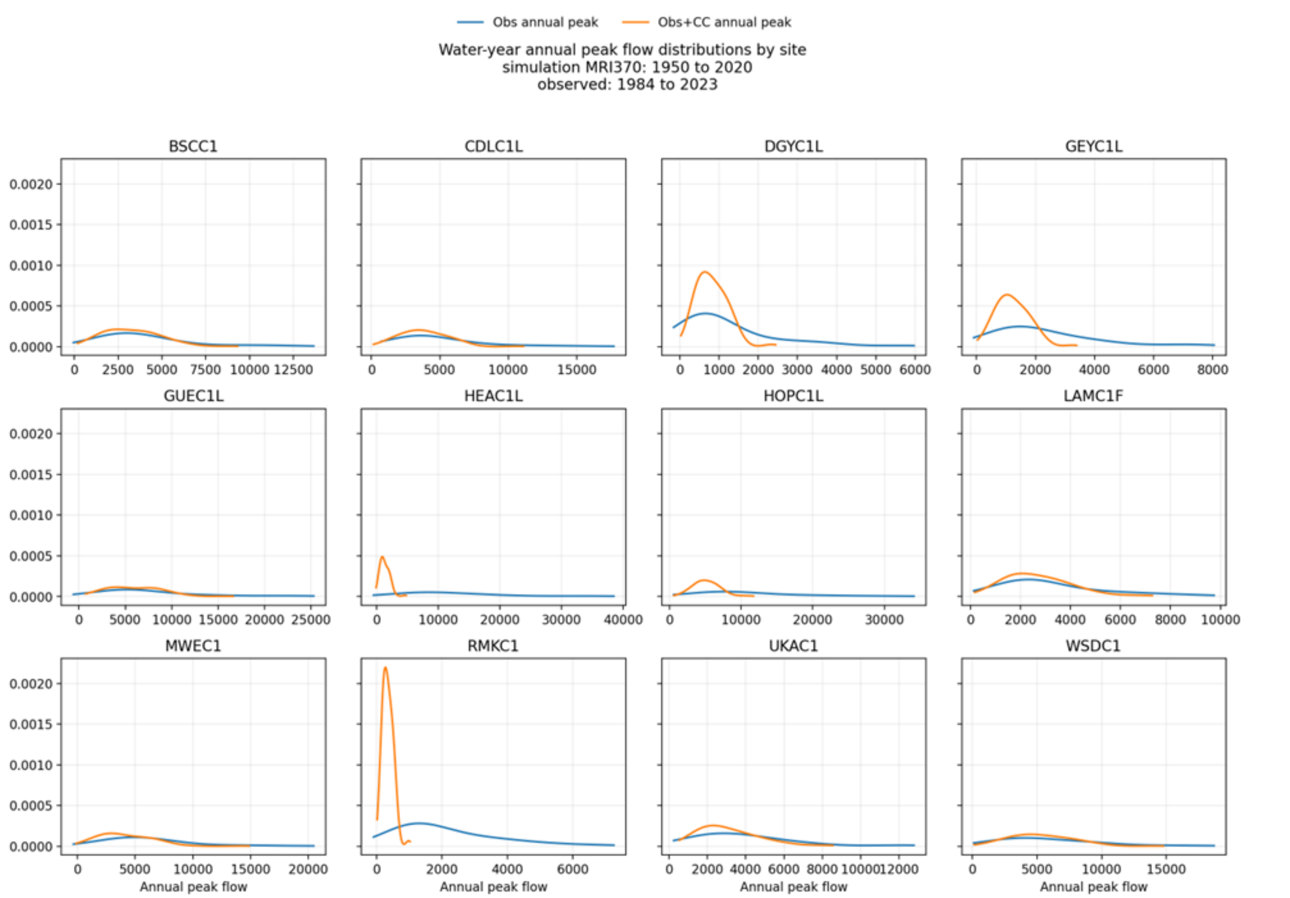

These baseline distributional differences in streamflow propagate into the baseline skill of the synthetic forecasts at these sites. For example, Figures H1-10 and H1-11 show the distributions of CRPS by lead time for WSDC1 and HOPC1L, respectively, both for the original HEFS hindcasts over the historical record and the synthetic forecasts applied to the baseline (1950 to 2020) period from the MRI-based hydrologic simulations. For Lake Sonoma inflow (WSDC1), the synthetic forecasts generally preserve the lead-dependent structure in CRPS distributions, and any differences remain relatively small. In contrast, at HOPC1L, where the mismatch in annual peak flows is more prominent (Figure H1-9), the contrast is much more pronounced. Here, the synthetic CRPS values are substantially lower than those from HEFS across all leads. This is consistent with the annual peak flow comparison, which suggests that the MRI baseline underrepresents larger events at HOPC1L, which leads to more accurate synthetic forecasts (i.e., lower CRPS values) as compared to those seen in HEFS and the observed streamflow record. In general, those sites with more similar flow distributions between baseline model and observed records (BSCC1, CDLC1L, GUEC1L, MWEC1, UKAC1, LAMC1F, WSDC1) exhibit CRPS distributions very similar to HEFS, while those sites with more substantial differences in flow distributions (DGYC1L, GEYC1L, HEAC1L, HOPC1L, RMKC1) exhibit CRPS distributions for the MRI-simulation that deviate meaningfully from those observed in HEFS.

Figure H1-10. Comparison of CRPS Distributions for HEFS Hindcasts for WSDC1 over the Historical Period and Synthetic Forecasts for the Baseline (1950-2020) Simulation from the MRI-based Scenario

(CRPS distributions are shown over the 100 largest flow events for WSDC1 [Lake Sonoma inflow]. Synthetic forecasts are summarized across 20 independent stochastic samples. The solid dot shows the mean CRPS across events.)

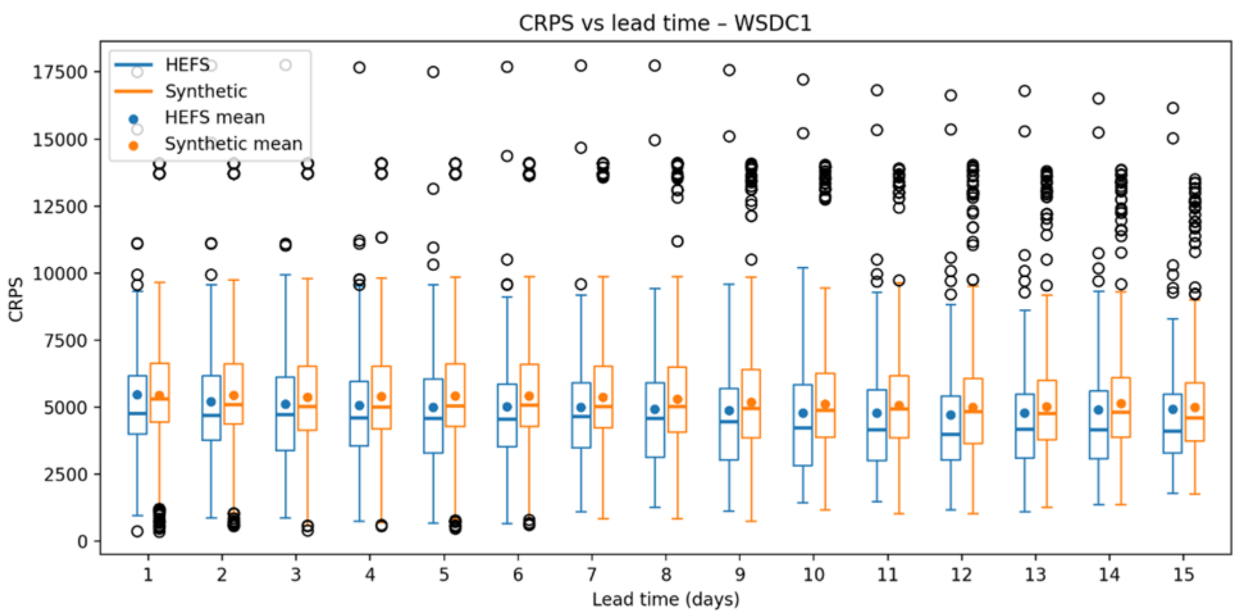

Figure H1-11. Comparison of CRPS Distributions for HEFS Hindcasts for HOPC1L over the Historical Period and Synthetic Forecasts for the Baseline (1950-2020) Simulation from the MRI-based Scenario

(CRPS distributions are shown over the 100 largest flow events for HOPC1L. Synthetic forecasts are summarized across 20 independent stochastic samples. The solid dot shows the mean CRPS across events.)

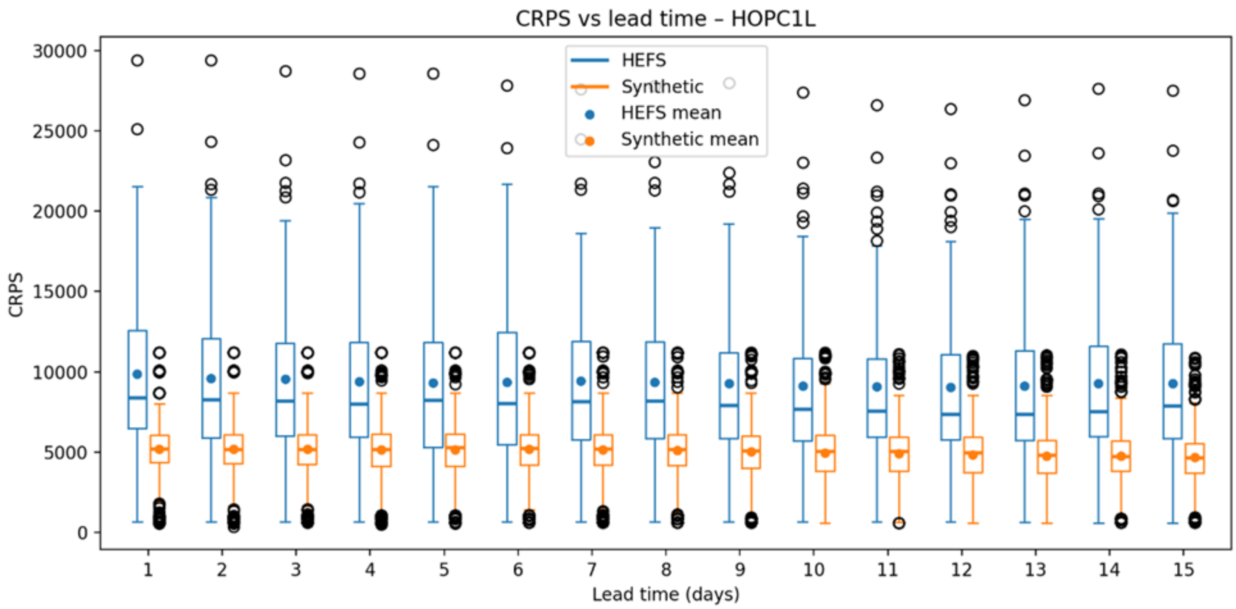

It is recognized that these distributional shifts may limit the realism of the synthetic forecasts at some locations. For that reason, it is recommended to rely primarily on the synthetic forecasts at the major inflow sites where baseline hydrology is better represented, while assuming perfect foresight for smaller downstream side inflows where the modeled marginal flow distributions depart more significantly from observations. Nonetheless, with this recommendation in mind, 20 synthetic forecast samples were generated for the full future period (1950 to 2100) at all sites and for all four climate model scenarios (ACC: SSP3-7.0; CNR: SSP2-4.5; IPS: SSP2-4.5, and MRI: SSP3-7.0) in order to maintain a complete systemwide synthetic forecast dataset.

To illustrate the character of the synthetic forecasts under future climate conditions, Figures H1-12 and H1-13 show example ensemble forecasts for two major inflow sites and flood events (Lake Sonoma in January 2050 and Lake Mendocino in December 2085), focusing on the MRI: SSP3-7.0 scenario. In both cases, the synthetic forecasts generate plausible ensembles around the target future hydrograph, while also showing substantial variation across samples and forecast lead times. At short lead times, the ensembles tend to align more closely with the timing and magnitude of the projected peak; however, at longer leads, the forecasts show greater spread and more variability in both peak magnitude and timing. This behavior is consistent with the intended design of the synthetic forecasting approach, which preserves lead-dependent forecast uncertainty observed in HEFS while transferring historical forecast error structure to future flow sequences.

Figure H1-12. Example Time Series of Synthetic Ensemble Forecasts for the January 2050 Flood into Lake Sonoma, as Simulated Under the MRI – SSP3-7.0 Scenario

(The two rows show synthetic forecast ensembles from two different stochastic samples, with each column displaying 1-, 4-, and 7-day ahead ensemble forecasts.)

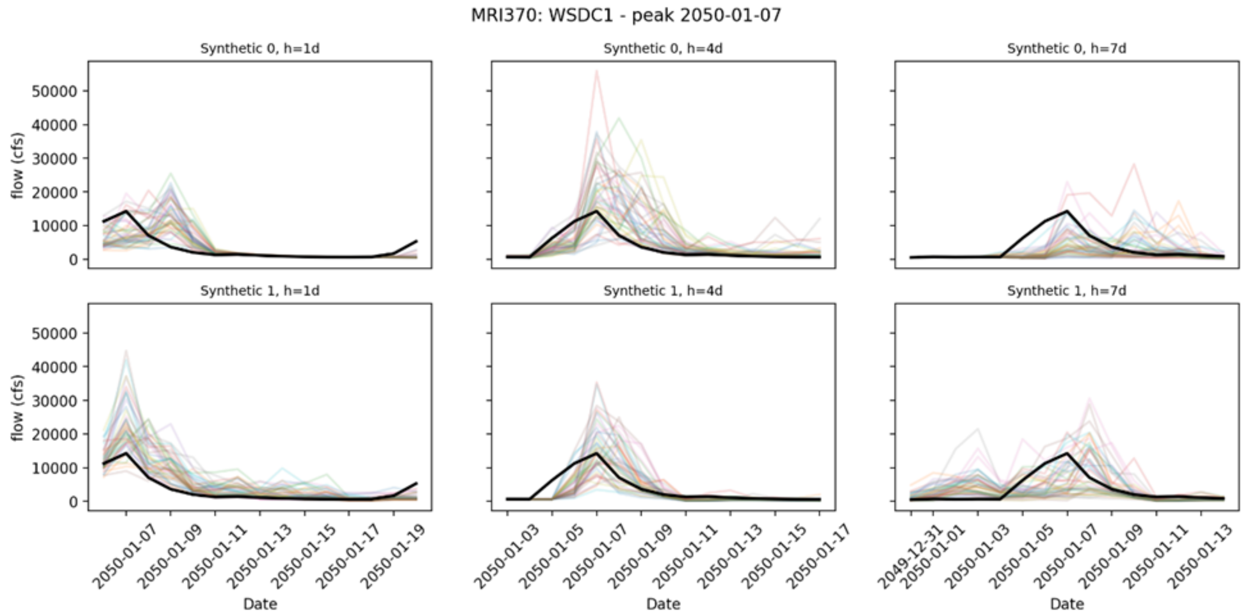

Figure H1-13. Example Time Series of Synthetic Ensemble Forecasts for the December 2085 Flood into Lake Mendocino, as Simulated Under the MRI – SSP3-7.0 Scenario

(The two rows show synthetic forecast ensembles from two different stochastic samples, with each column displaying 1-, 4-, and 7-day ahead ensemble forecasts.)

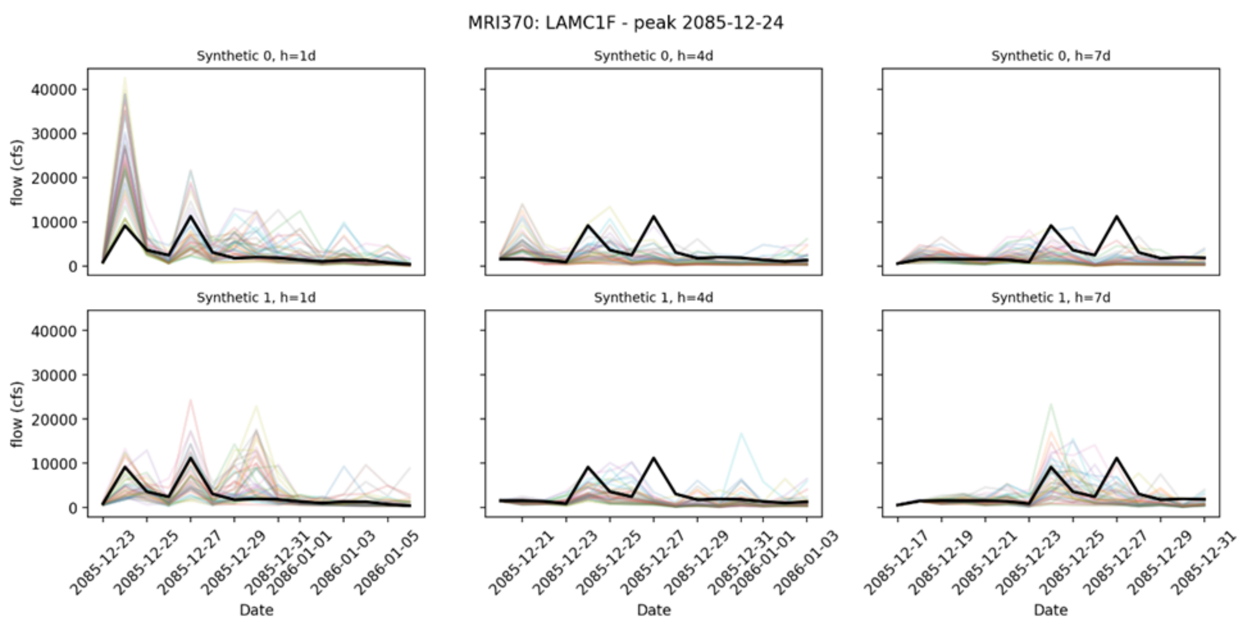

Finally, the following is examined: how the distribution of CRPS values for synthetic forecasts applied to future period (2070 to 2100) flows at all sites compares to historically observed CRPS distributions from the hindcast. Figure H1-14 shows an example of this for Lake Sonoma. Here, the distribution of CRPS values from the synthetic forecasts are modestly biased low compared to HEFS at all leads. In contrast, under the baseline (1950 to 2020) period, CRPS values from the synthetics were biased high compared to HEFS (Figure H1-10). This suggests that the impacts of climate change altered the distribution of flows at Lake Sonoma between the baseline and future periods, thereby changing the profile of synthetic forecast skill for the two periods.

Figure H1-14. Comparison of CRPS Distributions for HEFS Hindcasts over the Historical Period and Synthetic Forecasts for the Future (2070–2100) Simulation from the MRI-based Scenario

(CRPS distributions are shown over the 100 largest flow events for WSDC1 [Lake Sonoma inflow]. Synthetic forecasts are summarized across 20 independent stochastic samples. The solid dot shows the mean CRPS across events.)

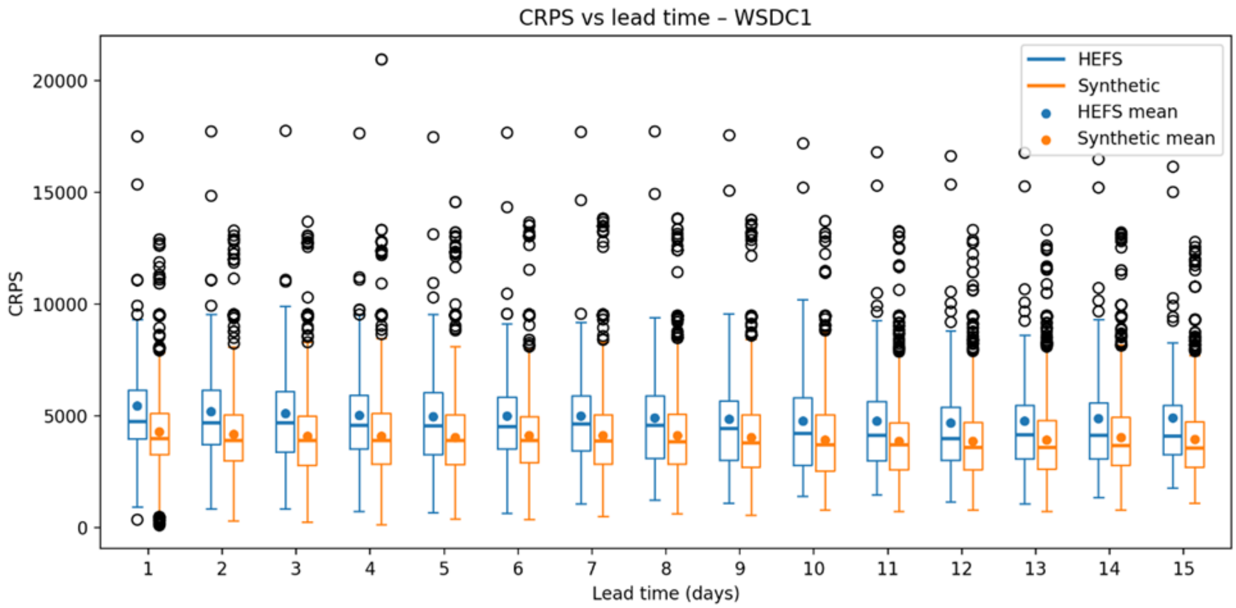

Taken together, these results demonstrate that the synthetic forecasting framework produces realistic forecast ensembles for future periods, both on an event basis and in aggregate, which can adapt to shifts in hydrology that emerge under climate change. This is important for the FIRO vulnerability analysis, since operational performance depends not only on the underlying hydrologic changes, but also on the uncertainty structure of the forecasts available to guide reservoir decisions.

H1.5 Conclusions

This technical memo demonstrates that synthetic ensemble streamflow forecasts can provide a practical and credible way to extend FIRO analysis to climate-informed future conditions in the Russian River system. Using hindcasts and observed inflows from 12 locations in the basin, including the key FIRO reservoirs at Lake Sonoma and Lake Mendocino, the synthetic forecasting approach was shown to reproduce features of HEFS behavior that are directly relevant for reservoir operations. These include the lead-dependent distribution of CRPS, the broad structure of ensemble reliability reflected in cumulative rank histograms, and the spatial correlation of forecast skill across sites in the Russian River watershed. Example historical events further showed that the synthetic forecasts generate realistic alternative realizations of forecast uncertainty for the kinds of flood events that matter most for system operations, rather than attempting to recreate any one historical hindcast exactly. Taken together, these results indicate that the synthetic forecasting model can preserve the essential probabilistic behavior of HEFS while extending that behavior to events and periods for which hindcasts are unavailable.

Application of the approach to climate projection-based streamflow traces shows both the promise and the limits of this framework for climate vulnerability assessment. At major inflow sites such as Lake Sonoma and Lake Mendocino, where the modeled baseline hydrology compares reasonably well with observations, the synthetic forecasts produce plausible future ensemble behavior that can support FIRO stress testing under nonstationary conditions. At some smaller downstream locations, however, shifts between modeled baseline and observed flow distributions suggest that synthetic forecast realism is lower, and results at those sites should be interpreted more cautiously. For this reason, the recommendation is to focus use of the synthetic forecasts on the major inflow locations and treat smaller side inflows with perfect foresight where appropriate in the operations analysis. With that framing, the synthetic forecast dataset developed here provides an important foundation for evaluating the robustness of FIRO in the Russian River Basin to climate change, including how FIRO benefits may persist or weaken under altered future hydrologic regimes.

H1.6 References

Brodeur, Z.P., W. Taylor, J.D. Herman, and S. Steinschneider (Brodeur et al.). 2025. “Synthetic Ensemble Forecasts: Operations-based Evaluation and Inter-model Comparison for Reservoir Systems across California”. *Water Resources Research*. 61, e2024WR039324. https://doi.org/10.1029/2024WR039324.

Kim, S., and D. Seo. 2025. “Improving Ensemble Precipitation and Streamflow Forecasts for Large Events with the Conditional Bias-Penalized Regression-Aided Meteorological Ensemble Forecast Processor.” *Weather and Forecasting*. 40, 959–975. https://doi.org/10.1175/WAF-D-24-0142.1.

Addendum H-1a. Historical Verification of Synthetic Forecasts

Figure H1a-1. Comparison of CRPS Distributions for HEFS Hindcasts and Synthetic Forecasts by Lead Time over the 100 Largest Flow Events in the Historical Hindcast Period for BSCC1

(Synthetic forecasts are summarized across 20 independent stochastic samples. The solid dot shows the mean CRPS across events.)

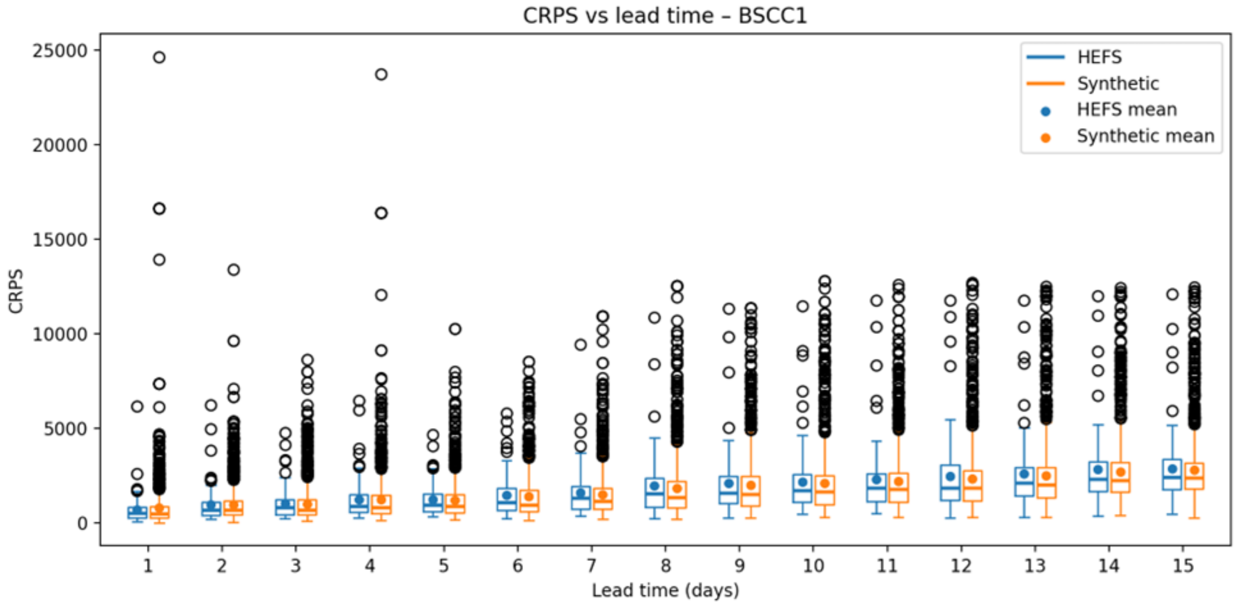

Figure H1a-2. Comparison of CRPS Distributions for HEFS Hindcasts and Synthetic Forecasts by Lead Time over the 100 Largest Flow Events in the Historical Hindcast Period for CDLC1L

(Synthetic forecasts are summarized across 20 independent stochastic samples. The solid dot shows the mean CRPS across events.)

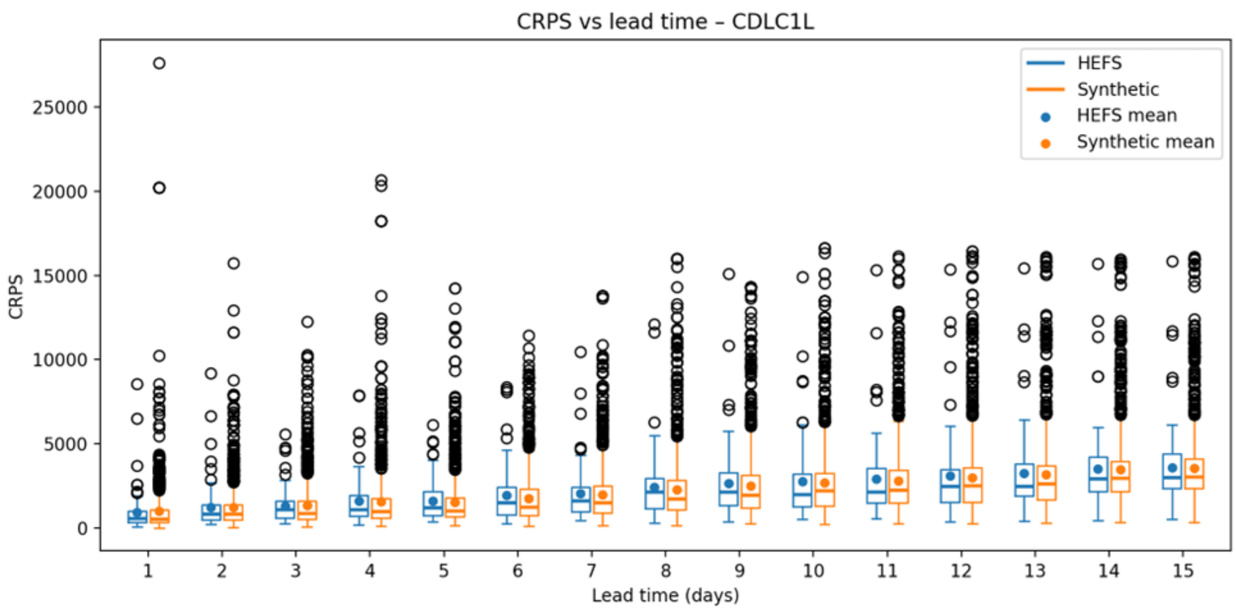

Figure H1a-3. Comparison of CRPS Distributions for HEFS Hindcasts and Synthetic Forecasts by Lead Time over the 100 Largest Flow Events in the Historical Hindcast Period for DGYC1L

(Synthetic forecasts are summarized across 20 independent stochastic samples. The solid dot shows the mean CRPS across events.)

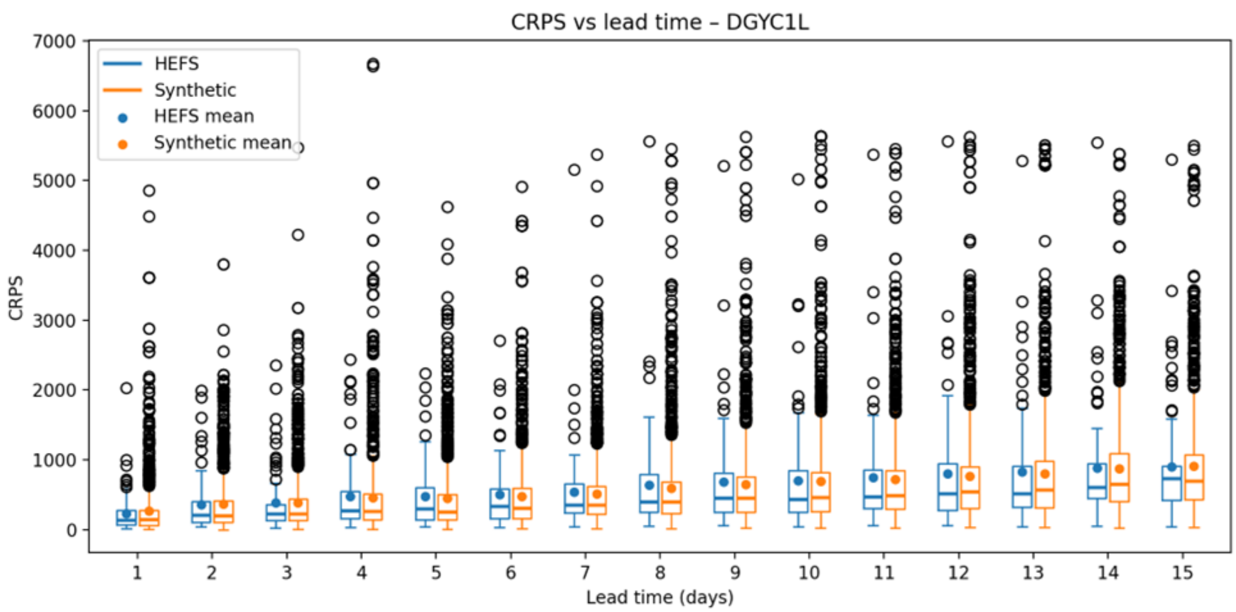

Figure H1a-4. Comparison of CRPS Distributions for HEFS Hindcasts and Synthetic Forecasts by Lead Time over the 100 Largest Flow Events in the Historical Hindcast Period for GEYC1L

(Synthetic forecasts are summarized across 20 independent stochastic samples. The solid dot shows the mean CRPS across events.)

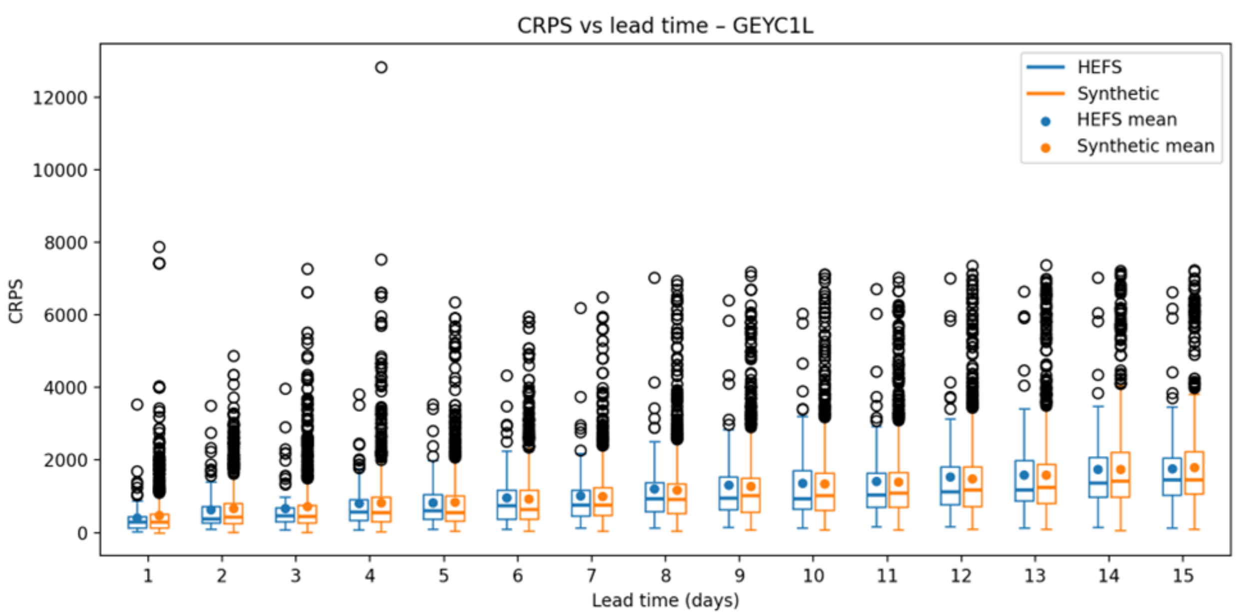

Figure H1a-5. Comparison of CRPS Distributions for HEFS Hindcasts and Synthetic Forecasts by Lead Time over the 100 Largest Flow Events in the Historical Hindcast Period for GUEC1L

(Synthetic forecasts are summarized across 20 independent stochastic samples. The solid dot shows the mean CRPS across events.)

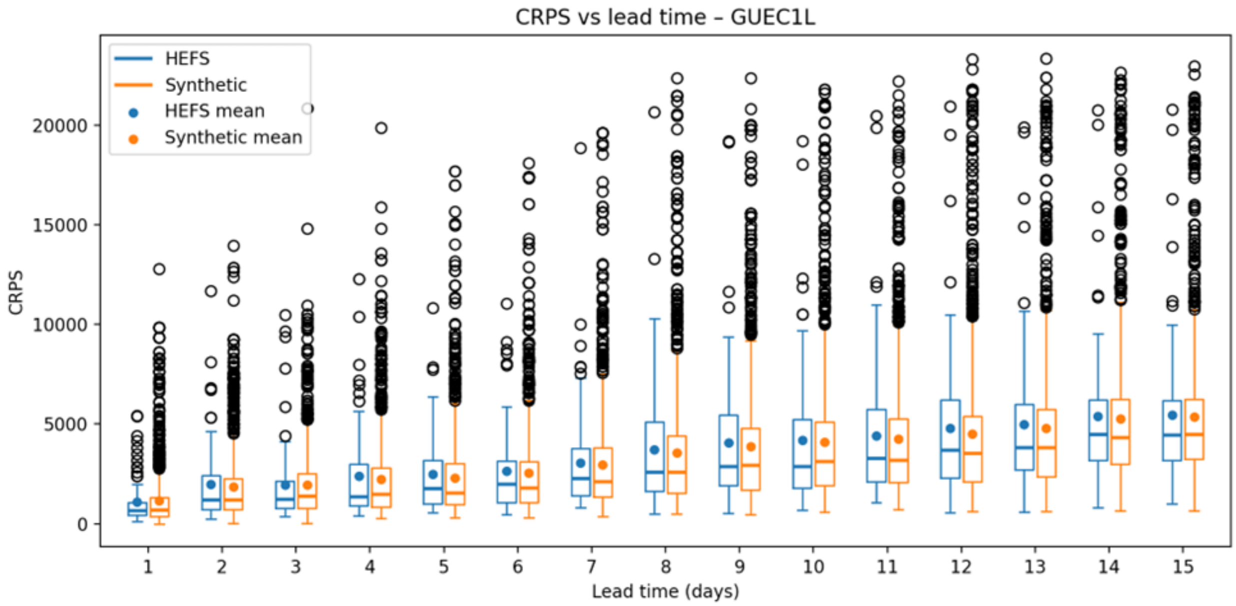

Figure H1a-6. Comparison of CRPS Distributions for HEFS Hindcasts and Synthetic Forecasts by Lead Time over the 100 Largest Flow Events in the Historical Hindcast Period for HEAC1L

(Synthetic forecasts are summarized across 20 independent stochastic samples. The solid dot shows the mean CRPS across events.)

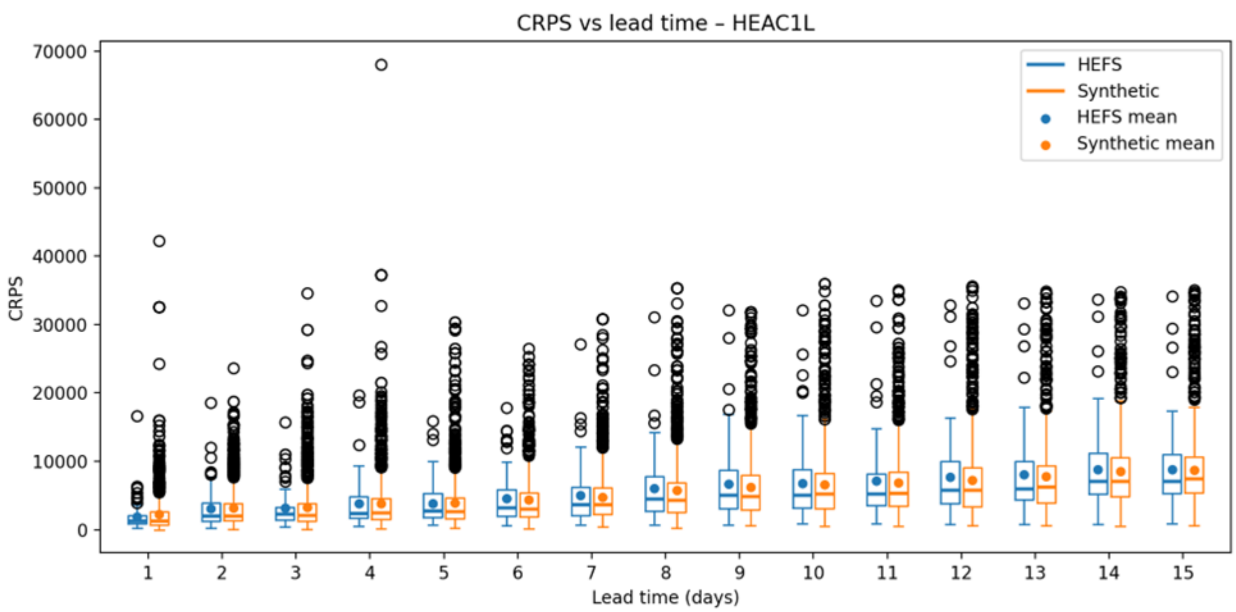

Figure H1a-7. Comparison of CRPS Distributions for HEFS Hindcasts and Synthetic Forecasts by Lead Time Over the 100 Largest Flow Events in the Historical Hindcast Period for HOPC1L

(Synthetic forecasts are summarized across 20 independent stochastic samples. The solid dot shows the mean CRPS across events.)

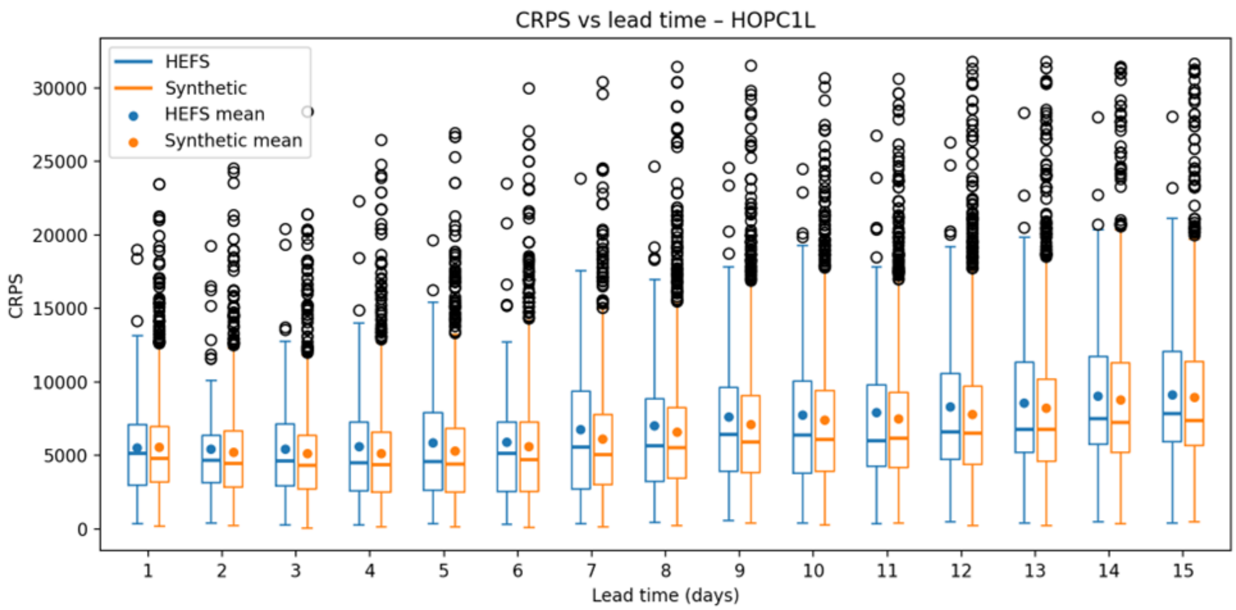

Figure H1a-8. Comparison of CRPS Distributions for HEFS Hindcasts and Synthetic Forecasts by Lead Time over the 100 Largest Flow Events in the Historical Hindcast Period for MWEC1

(Synthetic forecasts are summarized across 20 independent stochastic samples. The solid dot shows the mean CRPS across events.)

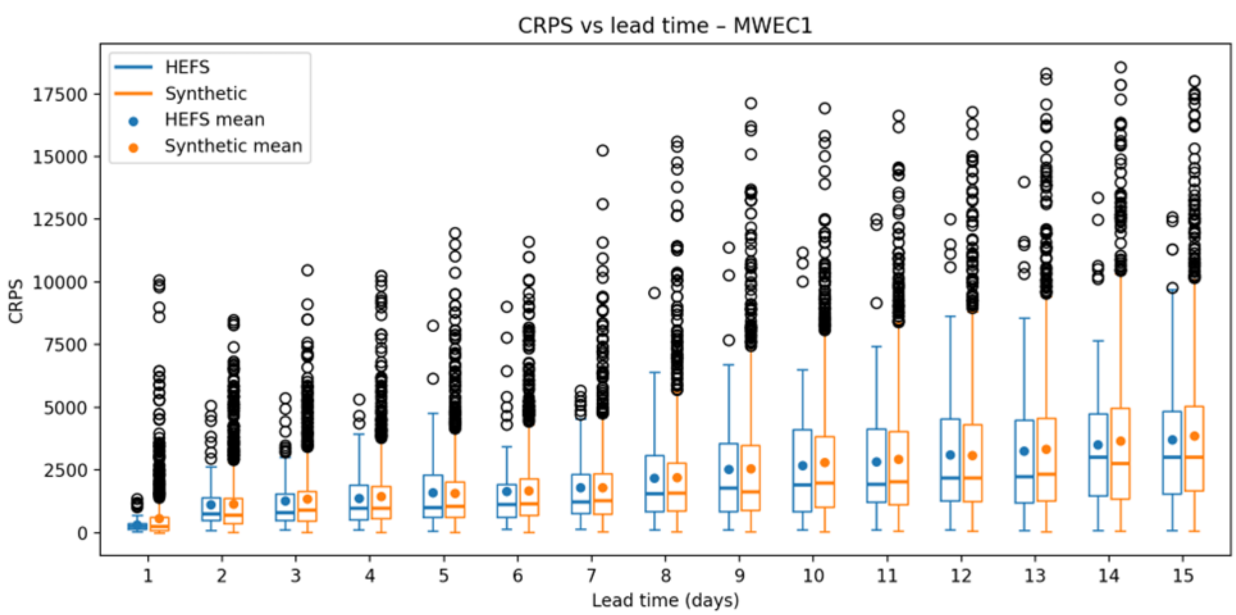

Figure H1a-9. Comparison of CRPS Distributions for HEFS Hindcasts and Synthetic Forecasts by Lead Time over the 100 Largest Flow Events in the Historical Hindcast Period for RMKC1

(Synthetic forecasts are summarized across 20 independent stochastic samples. The solid dot shows the mean CRPS across events.)

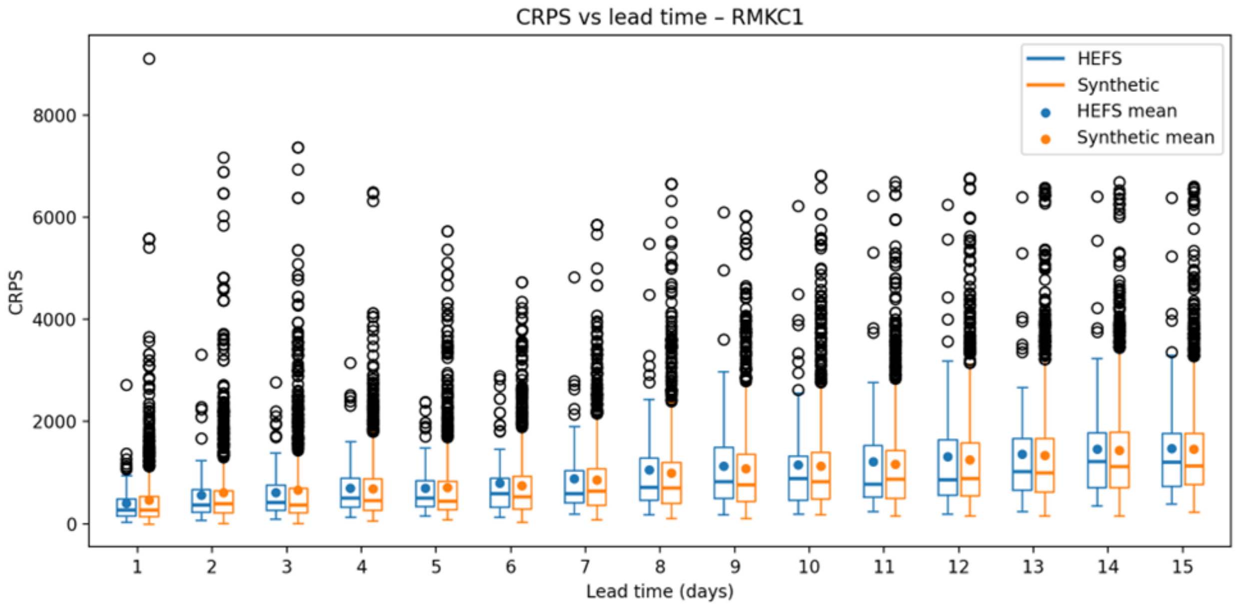

Figure H1a-10. Comparison of CRPS Distributions for HEFS Hindcasts and Synthetic Forecasts by Lead Time over the 100 Largest Flow Events in the Historical Hindcast Period for UKAC1

(Synthetic forecasts are summarized across 20 independent stochastic samples. The solid dot shows the mean CRPS across events.)

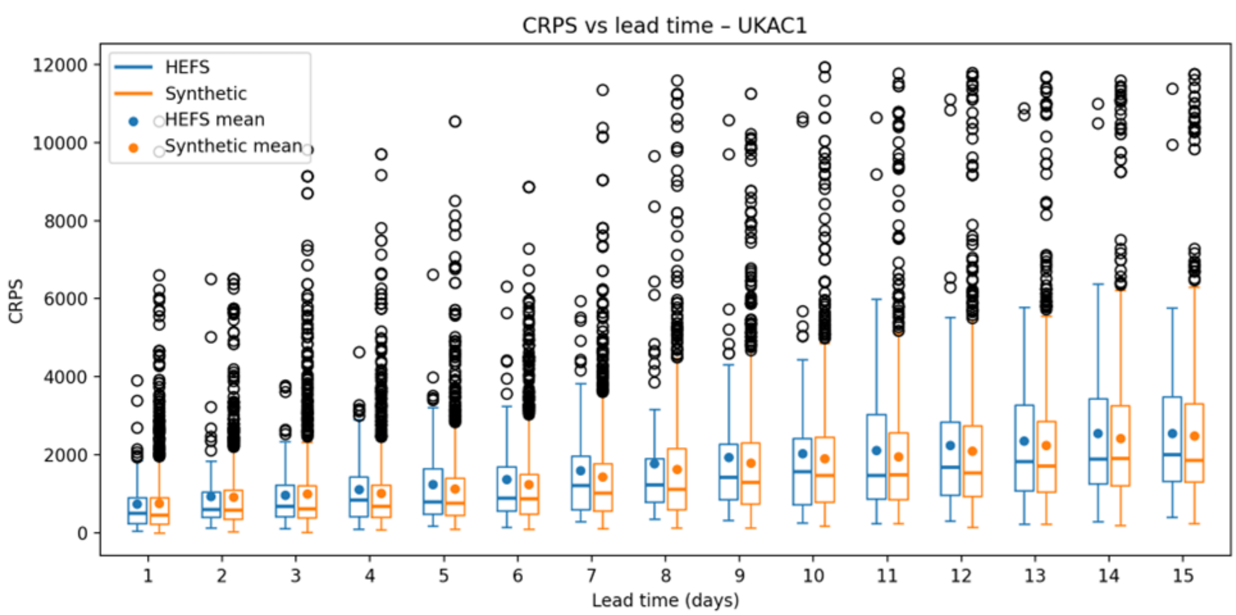

Figure H1a-11. Cumulative Rank Histograms by Lead Time for HEFS Hindcasts and Synthetic Forecasts over the 100 Largest Flow Events in the Historical Hindcast Period for BSCC1

(For the synthetic forecasts, a range of results are shown across 20 independent stochastic samples.)

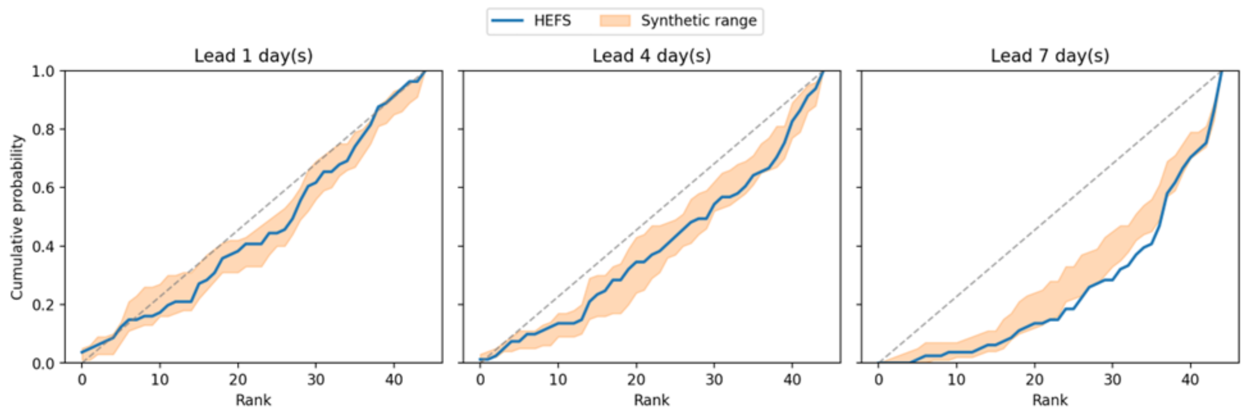

Figure H1a-12. Cumulative Rank Histograms by Lead Time for HEFS Hindcasts and Synthetic Forecasts over the 100 Largest Flow Events in the Historical Hindcast Period for CDLC1L

(For the synthetic forecasts, a range of results are shown across 20 independent stochastic samples.)

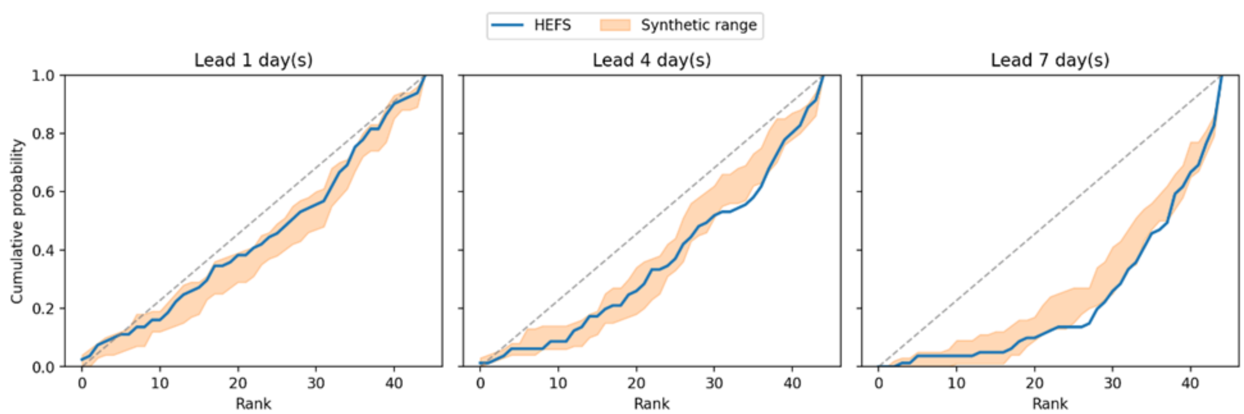

Figure H1a-13. Cumulative Rank Histograms by Lead Time for HEFS hindcasts and Synthetic Forecasts over the 100 Largest Flow Events in the Historical Hindcast Period for DGYC1L

(For the synthetic forecasts, a range of results are shown across 20 independent stochastic samples.)

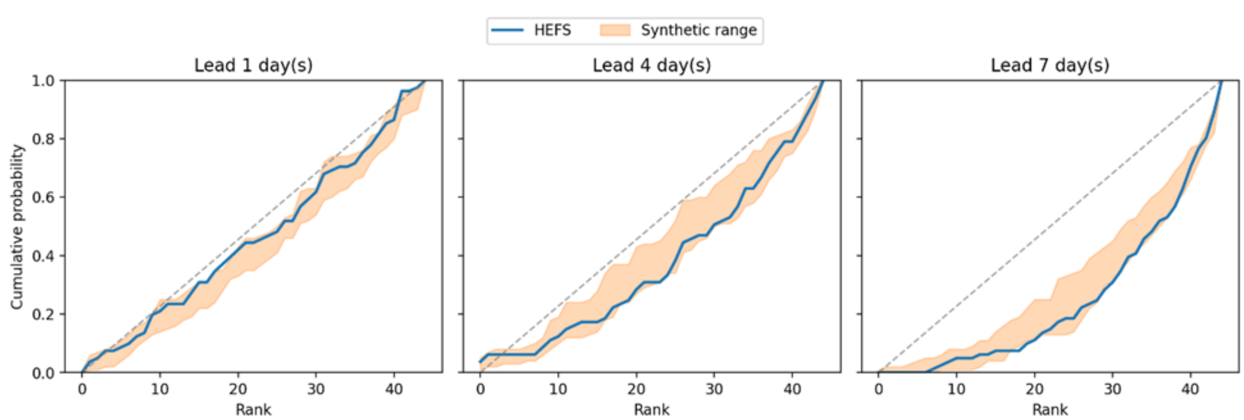

Figure H1a-14. Cumulative Rank Histograms by Lead Time for HEFS Hindcasts and Synthetic Forecasts over the 100 Largest Flow Events in the Historical Hindcast Period for GEYC1L

(For the synthetic forecasts, a range of results are shown across 20 independent stochastic samples.)

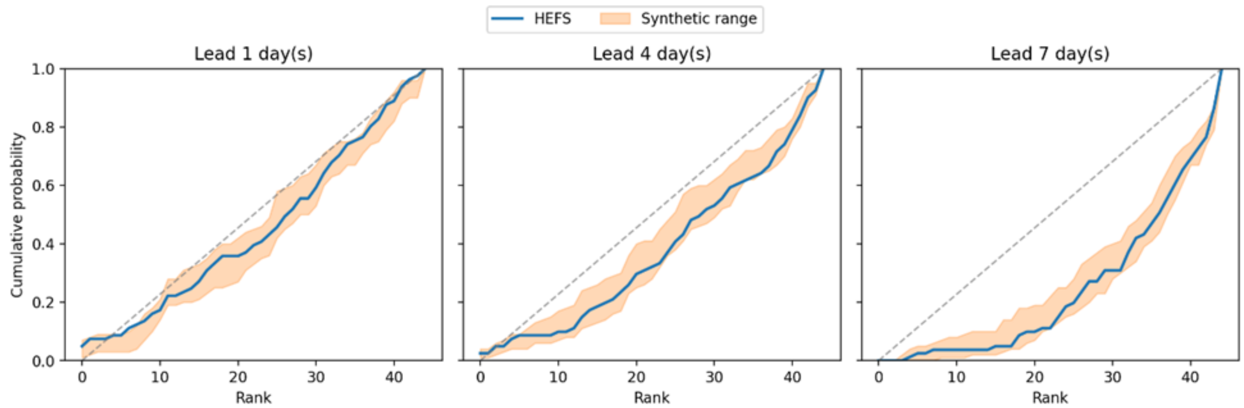

Figure H1a-15. Cumulative Rank Histograms by Lead Time for HEFS Hindcasts and Synthetic Forecasts over the 100 Largest Flow Events in the Historical Hindcast Period for GUEC1L

(For the synthetic forecasts, a range of results are shown across 20 independent stochastic samples.)

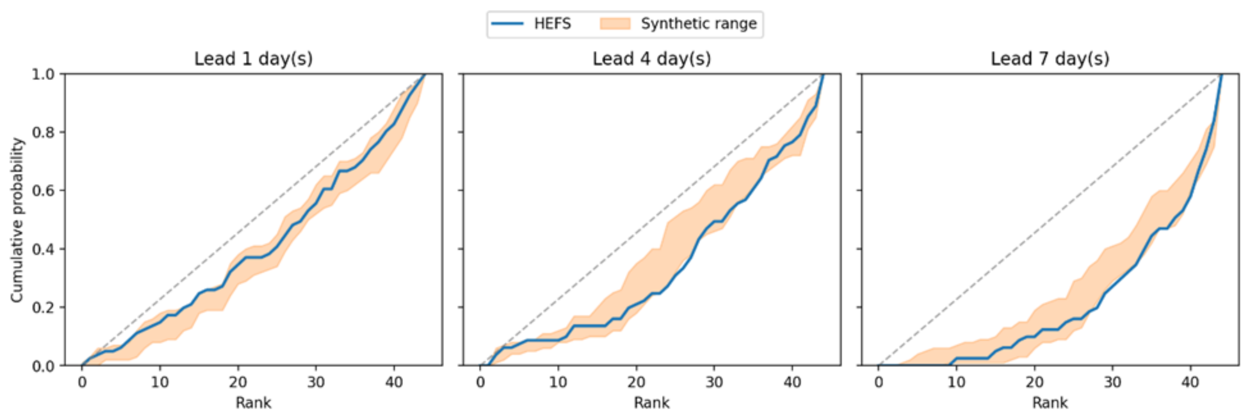

Figure H1a-16. Cumulative Rank Histograms by Lead Time for HEFS Hindcasts and Synthetic Forecasts over the 100 Largest Flow Events in the Historical Hindcast Period for HEAC1L

(For the synthetic forecasts, a range of results are shown across 20 independent stochastic samples.)

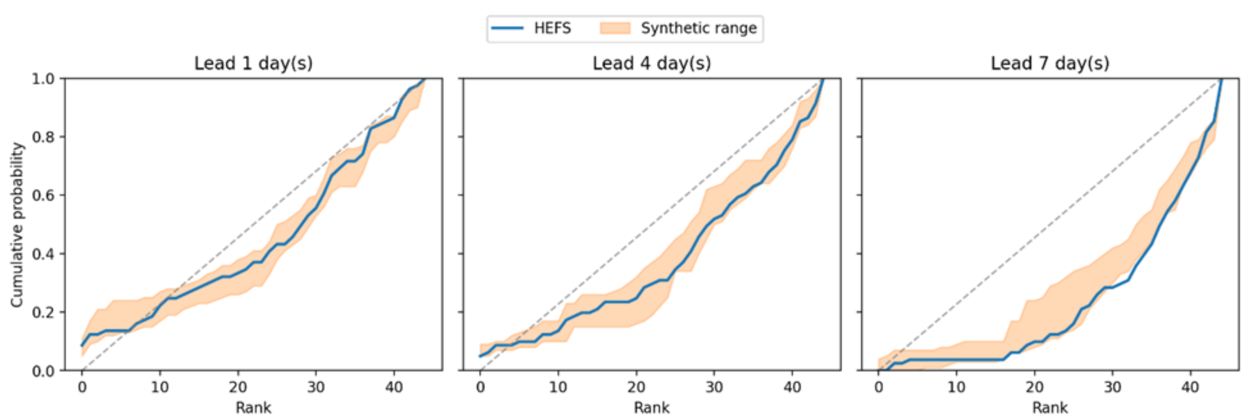

Figure H1a-17. Cumulative Rank Histograms by Lead Time for HEFS Hindcasts and Synthetic Forecasts over the 100 Largest Flow Events in the Historical Hindcast Period for HOPC1L

(For the synthetic forecasts, a range of results are shown across 20 independent stochastic samples.)

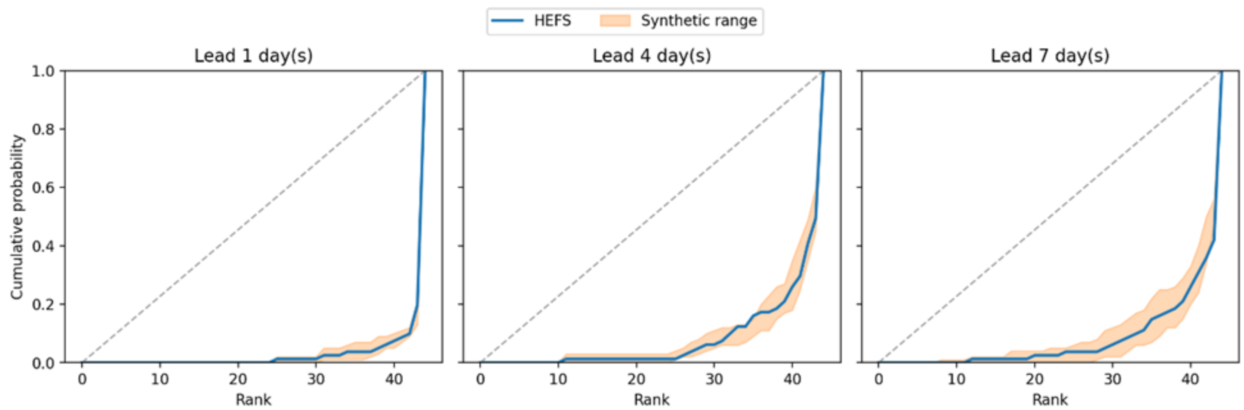

Figure H1a-18. Cumulative Rank Histograms by Lead Time for HEFS Hindcasts and Synthetic Forecasts over the 100 Largest Flow Events in the Historical Hindcast Period for MWEC1

(For the synthetic forecasts, a range of results are shown across 20 independent stochastic samples.)

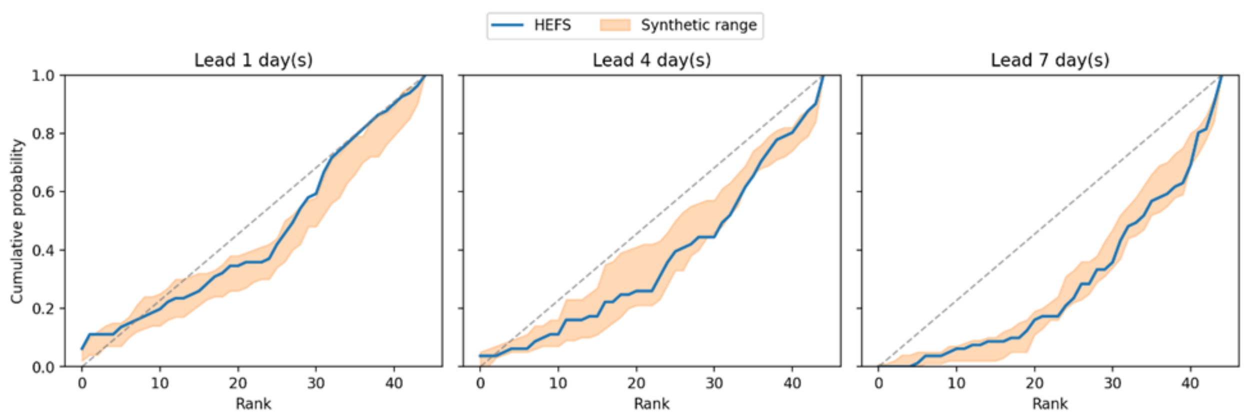

Figure H1a-19. Cumulative Rank Histograms by Lead Time for HEFS Hindcasts and Synthetic Forecasts over the 100 Largest Flow Events in the Historical Hindcast Period for RMKC1

(For the synthetic forecasts, a range of results are shown across 20 independent stochastic samples.)

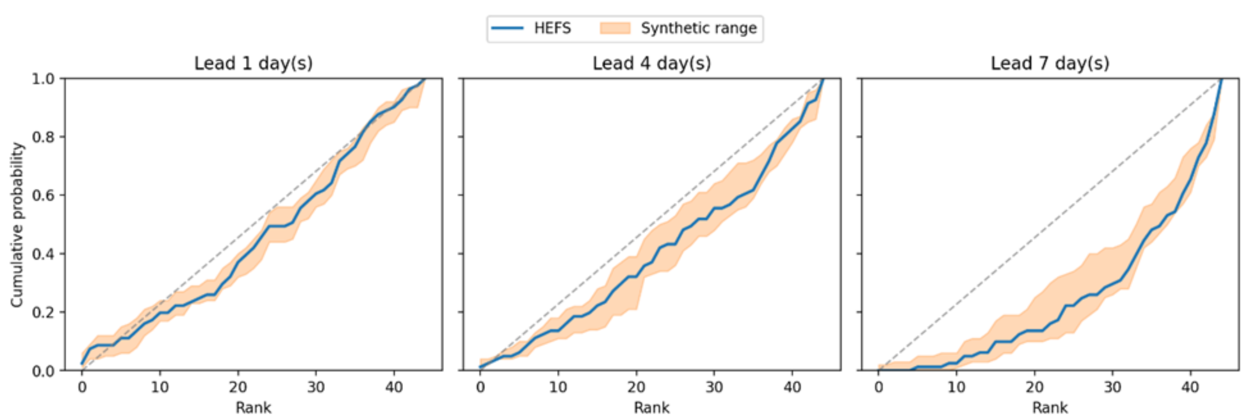

Figure H1a-20. Cumulative Rank Histograms by Lead Time for HEFS Hindcasts and Synthetic Forecasts over the 100 Largest Flow Events in the Historical Hindcast Period for UKAC1

(For the synthetic forecasts, a range of results are shown across 20 independent stochastic samples.)